

## CHEMICAL VARIATION ALONG STRIKE IN FELDSPATHOIDAL ROCKS OF THE EASTERN ALKALIC BELT, TRANS-PECOS MAGMATIC PROVINCE, TEXAS AND NEW MEXICO

LEE S. POTTER\*

*Department of Geological Sciences C1140, The University of Texas at Austin, Austin, Texas 78712, U.S.A.*

### ABSTRACT

Subduction-induced magmatism produced a NW–SE-trending narrow alignment of phonolite and nepheline trachyte intrusions in the eastern Trans-Pecos region of Texas and New Mexico, known as the Eastern Alkalic Belt (EAB). This 400 km by 20 km belt of mantle-derived, low-volume, highly fractionated intrusions crosses the boundaries of two distinct basement provinces, the Grenville and Ouachita fronts. Intrusions within this belt display little variation in major-element compositions and isotopic ages ( $35 \pm 2$  Ma). Two distinct segments, labeled the NW and SE segments, can be delineated based on changes in chemical variation at the Grenville Front. Increased chemical variation also occurs within the lead isotope transition zone (PbTZ) of James & Henry (1993a, b) that is roughly coincident with the Ouachita Front. In terms of the chemistry of the EAB rocks, it is unclear if the PbTZ marks a distinct discontinuity in the basement. One tephrite intrusion is present in the SE segment and is a possible representative of parental melts. These rocks show no evidence of significant modification by subduction processes, nor of significant involvement with continental crust despite their genesis beneath thick continental crust and high degrees of differentiation. The normalized trace-element diagram of the EAB tephrite has a pattern like that of an ocean-island basalt (OIB), and it resembles patterns of the leucocratic EAB rocks. The chemical similarity to OIB is striking; it persists despite extensive differentiation. Heterogeneities within the asthenospheric source of the EAB are relatively minor in the area studied.

*Keywords:* igneous, hypabyssal, alkaline, phonolite, trachyte, tephrite, trace elements, Texas.

### SOMMAIRE

Un épisode de magmatisme lié à un milieu de subduction est responsable de la formation d'une ceinture étroite de massifs intrusifs de phonolite et de trachyte néphélinique, orientée de nord-ouest à sud-est dans la partie orientale de la région Trans-Pecos, au Texas et au Nouveau-Mexique. Il s'agit de la ceinture alcaline orientale, longue de 400 km sur une largeur de 20 km. Les venues de magma très fortement fractionné, en faibles volumes et issues du manteau, traversent deux provinces géologiques distinctes, soit celle du Grenville et celle de l'Ouachita. Ces massifs intrusifs ne montrent aucune variation importante dans leurs compositions en termes d'éléments majeurs ou dans leur âge ( $35 \pm 2$  Ma). On reconnaît toutefois deux segments distincts, ceux du nord-ouest et du sud-est, à partir de variations en composition qui ont lieu au front du Grenville. On voit aussi une augmentation de l'hétérogénéité en composition à la zone de transition dans les isotopes de plomb, décrite par James et Henry (1993a, b). Il n'est pas clair si cette zone de transition, qui coïncide approximativement avec le front de l'Ouachita, signale une discontinuité dans le socle. Un massif intrusif de tephrite a été repéré dans le segment du sud-est, et représenterait peut-être le magma parental. Ces roches ne montrent aucun signe de modification importante attribuable à un processus de subduction, ni d'implication importante de la croûte continentale, malgré leur point d'origine en dessous d'une épaisse croûte et leur degré avancé de différenciation. Le bilan des concentrations normalisées des éléments traces dans la tephrite de cette ceinture ressemble à ceux de basaltes d'îles océaniques, qui, à leur tour, ressemblent à ceux des roches leucocrates de cette ceinture. La ressemblance de ces suites avec celles des îles océaniques est frappante, et persiste malgré un taux de fractionnement poussé. Les hétérogénéités de la source asthénosphérique semblent assez subtiles dans cette région.

(Traduit par la Rédaction)

*Mots-clés:* igné, subvolcanique, alcalin, phonolite, trachyte, tephrite, éléments traces, Texas.

---

\* Present address: Geology Department, Phelps Dodge Morenci, Inc., 4521 Highway 191, Morenci, Arizona 85540, U.S.A.

## INTRODUCTION

Alkaline magmatism in the Trans-Pecos Magmatic Province (TPMP) of Texas and New Mexico has produced a linear belt of intrusions that crosses at least two major province boundaries in the basement (Potter 1992). Within the TPMP, the Eastern Alkalic Belt (EAB) consists of at least 33 small intrusive bodies of phonolite and nepheline trachyte, and one of tephrite, that are irregularly dispersed in a belt more than 400 km long but only about 20 km wide (Fig. 1). To date, no study has examined the EAB as a complete entity to determine the degree of chemical variation present along strike within the belt.

This study concerns a portion of the belt that extends from the Cornudas Mountains on the Texas – New Mexico border, to just east of Big Bend National Park, although silica-undersaturated intrusions extend beyond the Rio Grande to the Gulf of Mexico coast (Bloomfield & Cepeda-Davila 1973, Robin & Tournon 1978, Elias-Herrera *et al.* 1991). The EAB rocks are recognized as an extension of the Eastern Rocky Mountains Front Alkalic Belt (Lindgren 1915).

It is impossible that the melts tapped a single magma reservoir, yet major-element compositions of the EAB intrusions show only slight variation along strike within the belt (Barker 1987, Potter 1992, 1994), and published radiometric ages fall in the narrow range of  $35 \pm 2$  Ma (Barker *et al.* 1977, Henry & McDowell 1986, Henry *et al.* 1986, 1991, Lambert *et al.* 1988).

Processes and conditions that are expected to affect chemical composition at any given point along the trend are: initial composition of the source, degree of partial melting, degree and nature of fractionation, magma mixing, contamination by assimilation in a magma reservoir (in the lower crust or upper mantle), contamination by assimilation at the point of emplacement, and post-emplacement alteration. The dominant process controlling variation within an intrusion should be fractional crystallization and, to a lesser degree, contamination during and after emplacement. Magma mixing could also cause variation within an intrusion, but no evidence, such as resorption or reverse zoning, has been observed in the EAB intrusions. Other processes should contribute to variation between intrusions, but not within intrusions.

## GEOLOGICAL SETTING

The TPMP of Texas and New Mexico consists of silica-undersaturated to -oversaturated intrusive and extrusive rocks of Tertiary age in NW–SE alignment. The province is composed of roughly parallel belts of rocks with similar rock-types that grade from alkaline felsic rocks in the northeast to more metaluminous felsic rocks in the southwest, with mafic rocks dispersed throughout. The timing and distribution of Tertiary magmatism varied in response to a complex

sequence of stress reorientations that is well known (Barker 1977, 1987, Walton & Henry 1979, Price & Henry 1984, Price *et al.* 1986b, 1987). These rocks range in age from 48 to 16 Ma, with more felsic material produced in the range of 37 to 26 Ma (Barker *et al.* 1977, McDowell 1979, Parker & McDowell 1979, Henry & McDowell 1986, Henry *et al.* 1986). The southwest-to-northeast chemical gradation in the igneous province in Mexico and Texas was demonstrated by Barker (1979, 1987), McDowell & Clabaugh (1979) and Henry *et al.* (1991).

The TPMP parallels the inferred trench that marked subduction of the Farallon Plate approximately 1000 km to the SW, and much of the magmatism was certainly contemporaneous with Farallon subduction that occurred over the interval 120–30 Ma (Henry *et al.* 1991). The EAB rocks have chemical and lithologic similarities to continental rifts, such as the Kenya Rift (Barker 1977). However, the alkaline magmatism was not contemporaneous with melt production in the nearby Rio Grande Rift (Barker 1979). Orientations of dikes contemporaneous with EAB magmatism indicate that the region was subjected to weak NE–SW compression as Laramide contraction waned, as part of the transition to back-arc extension (Price & Henry 1984, Barker 1987, James & Henry 1991). A comparison to rocks of ocean-island affinity was made by Nelson & Nelson (1987) using limited trace-element data.

The tectonic history of the Trans-Pecos region is exceedingly complex, and is described in Muehlberger & Dickerson (1989, general), Mosher (1993, Precambrian), and Barker (1987) and Price *et al.* (1987, Tertiary magmatism). Three distinct basement provinces underlie the TPMP: (1) 1200 Ma and older rocks of the Debaca Terrane northwest of the Grenville Front (King & Flawn 1953, Denison & Hetherington 1969, Mosher 1993), (2) 1000 to 1330 Ma rocks of the Llano Terrane southeast of the Grenville Front (Flawn 1956, King & Flawn 1953, Patchett & Ruiz 1987, Walker 1992, Mosher 1993), and (3) rocks of "South American affinities" south of the Ouachita Front (see below).

The position of the Grenville Front is shown by Reed (1993), as interpolated by Mosher (unpubl. data) from outcrops, well data, and geophysical information; it crosses the EAB trend at ~130 km (Fig. 1). The Ouachita Front (Flawn *et al.* 1961) crosses the trend at ~290 km. James & Henry (1993a, b) located a zone of transitional Pb isotopic values (the PbTZ) that is 20 to 30 km wide and is located about 10 km SE of the Ouachita Front at ~300 to 320 km along the trend. They interpreted the PbTZ to be a basement discontinuity between less radiogenic North American cratonic rocks of the Proterozoic Llano Terrane to the northwest, and younger, more radiogenic Proterozoic or Paleozoic South American crust and possibly oceanic crust to the southeast that was accreted during

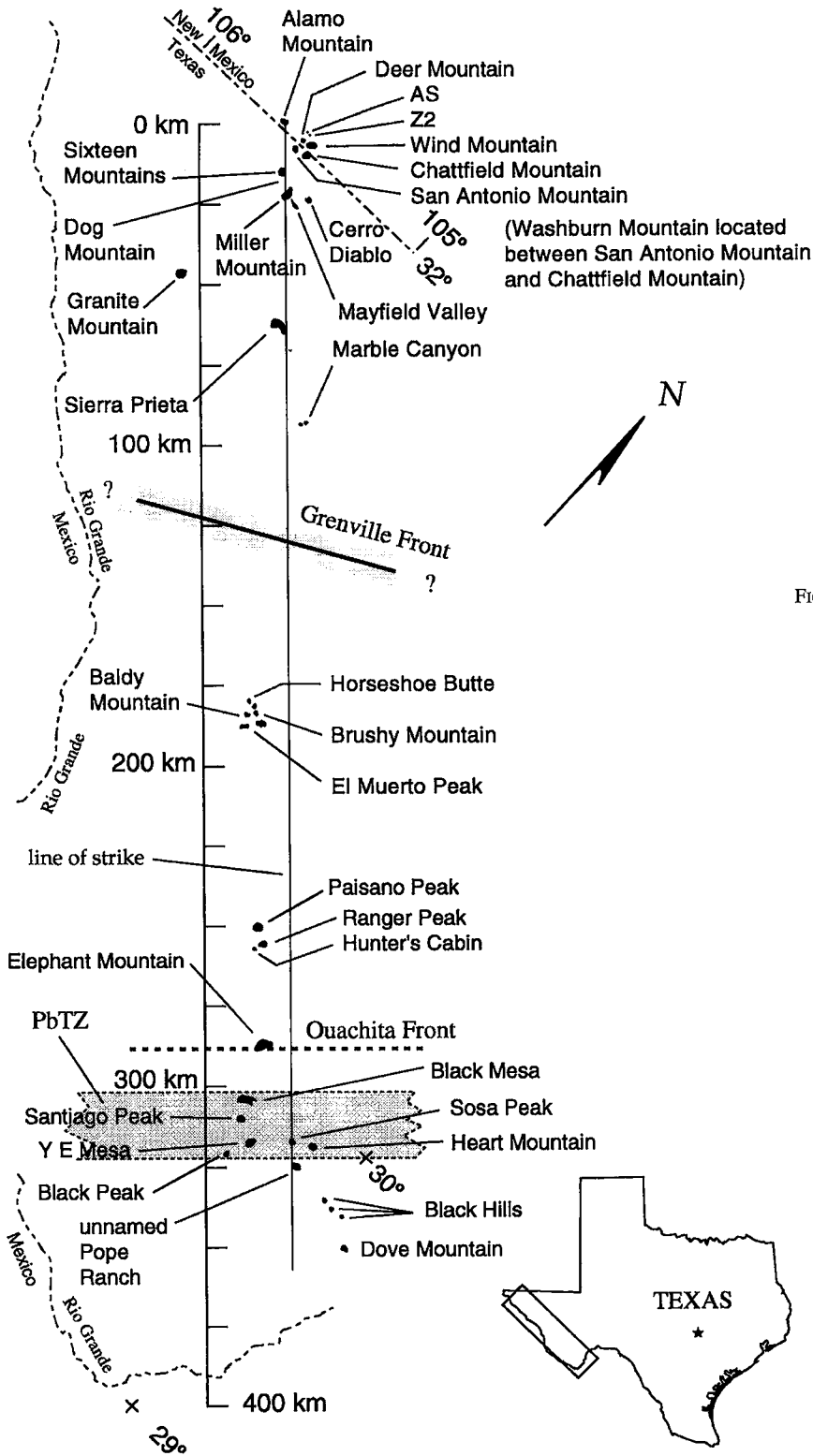


FIG. 1. Location of feldspathoidal EAB intrusions, strike line, and basement province boundaries. The location of the Grenville Front from Reed (1993) and Mosher (unpubl. data), of the Ouachita Front from Flawn *et al.* (1961), and of the lead isotope transition zone (PbTZ) of James & Henry (1993a, b).

the Ouachita Orogeny. Evidence of a Paleozoic arc is lacking in the Trans-Pecos; Handschy *et al.* (1987) suggested that the Ouachita deformational event was a result of compression from subduction to the *southeast*, and Goetz & Dickerson (1985) suggested that the basement southeast of the Ouachita Front may have North American affinities.

The Trans-Pecos region was covered by a broad, shallow platform that was stable through much of the Early Paleozoic. West Texas was repeatedly partitioned into basins and basement-cored uplifts, in the Late Pennsylvanian, Early Mesozoic, and Late Mesozoic – Early Tertiary (Laramide), with adjustments between blocks occurring each time. Platform carbonates were again deposited on uplifted basement blocks during the Cretaceous, and the EAB intrusions are hosted in either Permian or Cretaceous platform carbonates (except for intrusions within the Davis Mountains, which are hosted by Tertiary volcanic rocks).

#### ANALYTICAL METHODS

To insure that chemical variation along the EAB is a function of location and not interlaboratory variation, previously published analytical results were used only for elements and oxides considered not to be critical (such as  $\text{SiO}_2$ ,  $\text{Al}_2\text{O}_3$ ,  $\text{Fe}_2\text{O}_3^{\text{T}}$ ,  $\text{FeO}$ ,  $\text{H}_2\text{O}^+$ ,  $\text{H}_2\text{O}^-$ ,  $\text{CO}_2$ ), or where additional sample material was not available. Total iron as  $\text{Fe}_2\text{O}_3$  ( $\text{Fe}_2\text{O}_3^{\text{T}}$ ) is used to avoid the possible changes in valence state of iron caused by the vagaries of post-emplacement oxidation and sample preparation. A detailed description of analytical methods and precision for each element is found in Potter (1996) and has been submitted to the Depository of Unpublished Data (see below).

Samples were selected so as to cover the maximum observed range of compositions and petrographic variation of phonolite and nepheline trachyte, and analyzed samples were limited to rocks of silica-undersaturated to -saturated compositions. Strongly quartz-normative samples are assumed (*a priori*) to have suffered crustal contamination and are not part of the study. The diversity of the sample suite was restricted by the sampling biases in the pre-existing samples, problems with land access, and by the freshness of material (scree on Alamo Mountain was fresher than outcrop), and by my goal to sample "at least one of everything". Thus, only one sample was obtained for analysis from certain intrusions, and the suite should not be considered representative in the statistical sense.

#### CHEMICAL VARIATIONS

##### Major-element variation

The leucocratic EAB rocks exhibit very little variation in major-element concentration owing to the

high degree of differentiation that the magmas have undergone. Results of chemical analyses, CIPW normative calculations, and selected graphs are available from the Depository of Unpublished Data, CISTI, National Research Council of Canada, Ottawa, Ontario K1A 0S2. A subset of 13 samples with nearly complete trace-element suites is listed in Table 1. The names and location of all samples used are listed in Appendix 1.

The majority of the samples used in this study are fine-grained, porphyritic, shallow intrusive rocks. To facilitate comparison, samples have been classified in terms of total alkalis *versus* silica (TAS: Fig. 2) using the IUGS chemical classification for fine-grained igneous rocks. All but four samples plot in the phonolite and trachyte fields. Most rocks in the trachyte field contain modal or normative feldspathoids. Two coarse-grained samples from a small plug in the Cornudas Mountains plot in the trachyandesite field and were named "augite syenite" and later described as mugearite (Barker *et al.* 1977, Barker 1987). The name augite syenite will be retained, based on historical precedence, content of mafic minerals and grain size, and coincidence with the approximate TAS coordinates of syenite. One intrusion in the EAB trend is both sufficiently primitive and alkaline to be considered a possible mafic precursor to the phonolites. Two samples from it plot in the tephrite field. The differences between phonolite and nepheline trachyte are primarily those of definition, and separate symbols are not used on the following graphs.

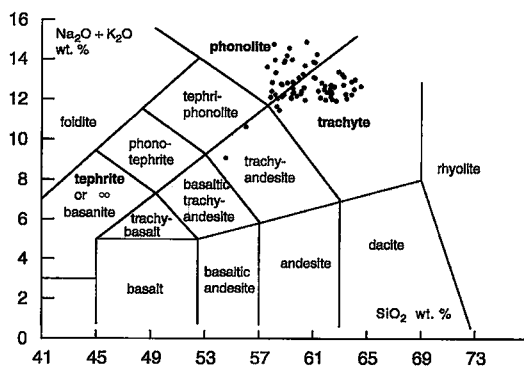


FIG. 2. TAS classification of EAB leucocratic rocks and tephrite (Le Maitre 1989). Solid symbols represent leucocratic rocks (phonolite, trachyte, augite syenite); open symbols represent tephrite. These symbols will be retained in most of the following figures.

TABLE 1. REPRESENTATIVE CHEMICAL COMPOSITIONS AND CIPW NORMS OF EAB ROCKS

Sample Distance	AL-11 0	AS-5 7	DM-5 18	CD-7 26	SP-39 65	J84-1 94	87103 188	PP-122 251	EM-903 288	BM-904 304	BP-901 321	UP-907 323	MBH-904 338
SiO <sub>2</sub> (%)	58.89	55.15	59.03	60.83	60.70	57.47	58.24	63.00	60.03	60.54	43.93	59.28	58.87
TiO <sub>2</sub>	0.17	1.51	0.11	0.22	0.08	1.45	0.13	0.51	0.37	0.13	3.79	0.12	0.22
Al <sub>2</sub> O <sub>3</sub>	18.43	18.41	17.81	17.62	17.68	17.13	18.77	17.00	17.29	16.65	15.99	16.60	17.67
Fe <sub>2</sub> O <sub>3</sub> T	4.57	6.28	5.10	6.29	5.87	7.35	6.07	4.48	5.48	4.98	12.59	4.58	6.40
Fe <sub>2</sub> O <sub>3</sub>	2.29	2.63	4.40	2.99	5.73	3.02	4.65	1.50	3.63	3.55	2.86	3.26	6.12
FeO	2.05	3.28	0.63	2.97	0.13	3.89	1.27	2.68	1.66	1.29	8.75	0.45	0.25
MnO	0.24	0.16	0.31	0.25	0.26	0.10	0.38	0.30	0.24	0.34	0.17	0.31	0.20
MgO	0.10	1.96	0.13	0.37	0.11	1.10	0.22	0.51	0.38	0.33	4.85	0.23	0.32
CaO	0.66	4.24	0.90	1.65	0.85	2.80	0.99	1.01	1.19	0.59	8.44	1.18	1.58
Na <sub>2</sub> O	9.33	6.01	8.28	6.71	8.75	6.25	8.90	7.17	6.30	8.46	4.84	7.27	6.41
K <sub>2</sub> O	5.17	4.44	5.15	5.21	4.97	5.77	5.09	4.89	5.66	4.40	2.12	5.01	5.86
P <sub>2</sub> O <sub>5</sub>	0.07	0.72	0.04	0.07	0.05	0.44	0.05	0.16	0.10	0.02	0.99	0.01	0.16
H <sub>2</sub> O+	1.35	0.76	1.92	1.20	1.02	0.85		0.58	1.27		2.21	2.35	1.43
H <sub>2</sub> O-	0.05	0.09	0.20	0.20	0.12		0.14	0.14	0.31	0.07	0.14	0.38	0.18
CO <sub>2</sub>	0.05	0.22	nil	0.42	0.07	0.18	0.03	0.06	0.02	0.13	0.06	0.21	0.21
Total	98.84	99.36	98.90	100.71	100.52	100.45	98.86	99.50	98.46	96.51	99.15	96.66	99.49
Sc (ppm)	0.6	4.4	0.7	3.5	10.0		3.3	18.1	14.6	0.9	19.2	0.8	6.1
V	77	180	66	50	78		38	57	41	70	117	72	43
Cu	35	9	19	28	23	21	18	12	7	29	47	17	16
Zn	213	76	246	181	262	70	199	152	95	409	80	344	146
Rb	194	92	191	159	248	85	187	82	71	352	34	317	144
Sr	48	1008	19	61	11	315	15	21	34	14	1044	71	42
Y	59	31	83	61	110	24	76	65	47	162	32	133	63
Zr	1626	524	1731	1441	1641	304	916	657	708	2033	342	1650	1571
Nb	248	98	311	190	291	42	252	110	106	556	44	463	166
Ba	63	1218	14	15	6	860	5	1019	50	20	522	73	171
Li	61	26	56	49	71		38	20	35	96	7	60	37
Cs	4.3	1.7	2.7	2.6	4.9	3	2.3	2.0	2.2	5.9	1.7	8.4	1.9
Hf	35	11	37	29	35	4.8	18	14	16	51	7.0	41	25
Ta	18	7.2	2.1	1.1	16	3.9	14	6.2	5.3	38	2.6	28	9.6
Th	40	14	38	23	28	4.7	22	10	9.6	71	4.5	55	14
U	12	3.6	9.8	6.4	8.4	1.5	4.9	2.5	2.4	21	1.7	9.8	2.2
La	137.6	74.1	163.7	120.5	175.2	58.2	174.7	91.6	84.7	330.4	48.6	276.4	94.1
Ce	233.7	141	289.9	235.1	307.9	130.2	304.1	163.8	149.8	376.1	107.1	433.8	159.8
Nd	76.8	58	100.6	79.4	120.5	61.1	110.2	70.1	63.7	169.8	54.1	162.7	69.0
Sm	9.3	96	14.4	10.3	19.2	10.0	14.3	10.8	8.6	25.0	10.6	21.2	11.1
Eu	1.18	1.2	0.82	0.79	1.04	2.72	1.73	2.88	1.20	2.16	3.66	1.95	1.68
Gd	8.69		11.96	9.81	16.01	8.98	13.67	9.59	8.45	20.26	9.39	19.64	9.34
Dy	7.99		11.93	9.27	16.47	6.64	13.50	9.48	7.94	20.23	7.03	19.60	8.62
Er	4.54		7.33	5.29	9.80	2.86	8.39	5.71	4.56	12.74	3.19	12.51	4.88
Yb	4.05	2.6	7.53	4.96	9.61	2.01	9.06	5.19	4.51	12.47	2.17	12.60	3.88
Lu	0.49	0.37	1.04	0.93	1.65	0.50	1.62	0.93	0.88	1.97	0.21	1.99	0.48
CIPW Norm													
or	30.54	26.24	30.42	30.81	29.37	34.10	30.06	28.90	33.46	26.01	12.55	29.62	34.65
ab	39.11	39.39	44.59	52.35	46.09	39.48	39.70	60.22	52.22	50.25	16.79	50.99	46.86
an		10.14		2.55		1.65			2.17		15.62		2.11
ne	14.59	6.21	9.95	2.42	9.31	7.27	15.46		0.60	5.90	13.10	3.52	4.02
ac	6.63		6.27		9.51		6.20	0.37		9.23		3.57	
ns	1.25												
wo			1.39		1.31		0.62		0.17			1.77	1.06
di-di	0.17	4.20	0.68	1.14	0.58	4.40	1.17	1.06	2.05	0.66	10.60	1.22	1.72
di-hd	2.33	1.24		3.36		3.41	1.42	2.54		1.72	5.92		
hy-en								0.12					
hy-fs								0.32					
ol-fo	0.12	2.06		0.27		0.49		0.46		0.37	5.02		
ol-fa	2.09	0.77		1.01		0.48		1.41		1.22	3.55		
mt		3.82	2.70	4.33	1.01	4.38	3.64	1.99	5.04	0.52	4.15	2.11	0.81
il	0.31	2.87	0.21	0.41	0.16	2.75	0.25	0.97	0.71	0.25	7.20	0.22	0.43
hm			0.37		1.74				0.16			0.57	5.56
ap	0.17	1.69	0.10	0.16	0.12	1.04	0.12	0.37	0.25	0.06	2.34	0.03	0.38
zr	0.33	0.11	0.35	0.29	0.33	0.06	0.18	0.13	0.14	0.41	0.07	0.33	0.32
Total	97.63	98.73	97.02	99.10	99.54	99.51	98.83	98.86	96.97	96.60	96.93	93.95	97.90
cc'	0.11	0.50	0.00	0.96	0.16	0.41	0.07	0.14	0.05	0.30	0.14	0.48	0.48
Na+K Al (mol)	1.14	0.80	1.08	0.95	1.12	0.96	1.07	1.00	0.95	1.12	0.64	1.05	0.96

Concentrations in italics by G. K. Hoops from Barker *et al.* (1977) and Price *et al.* (1986a); CIPW norms calculated without calcite; cc' is normative calcite. REE concentrations by ICP-AES, except AS-5: Tb = 1.6 ppm by INAA. BP-901: Cr = 23 ppm, Ni = 35 ppm.

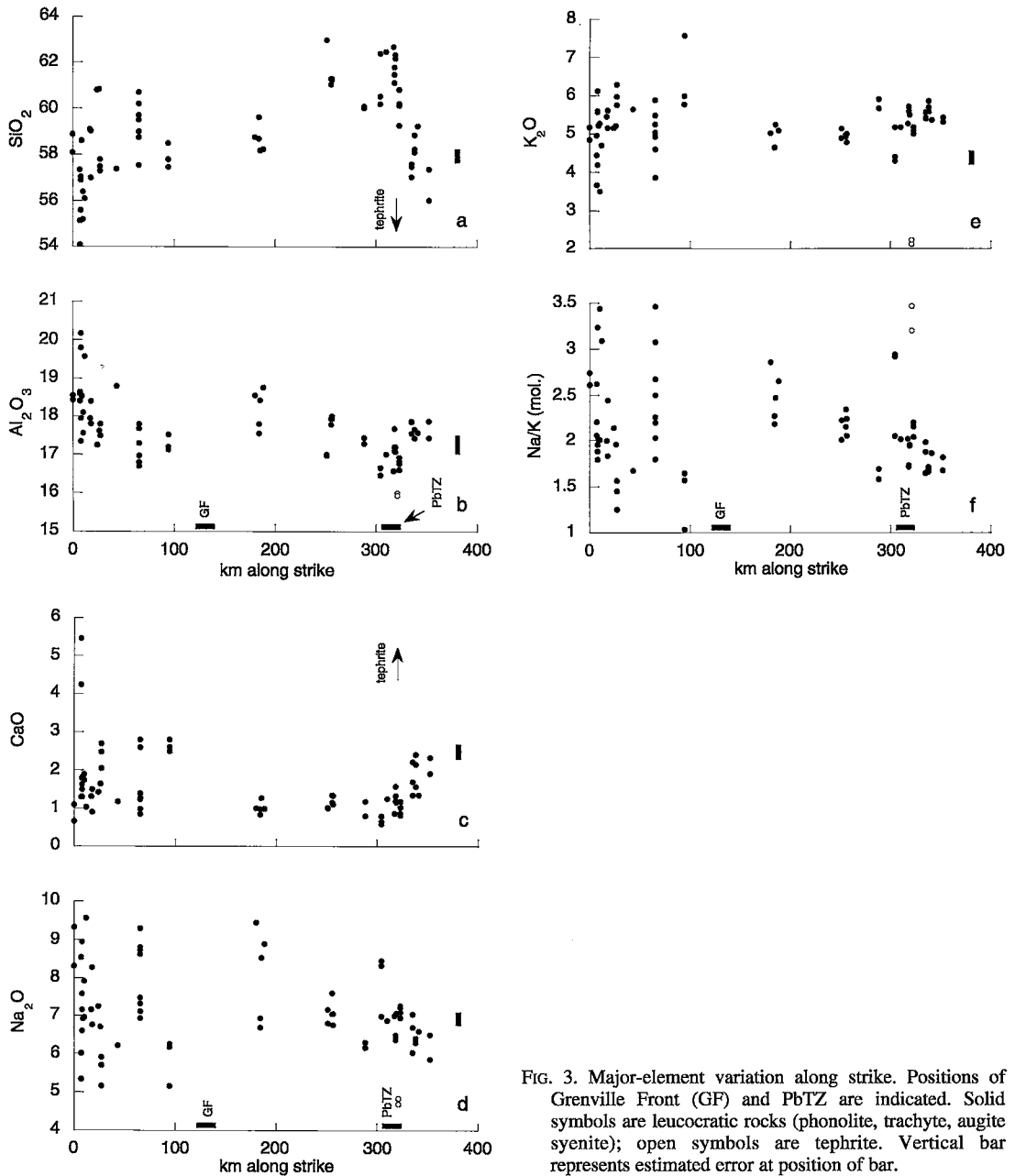


FIG. 3. Major-element variation along strike. Positions of Grenville Front (GF) and PbTZ are indicated. Solid symbols are leucocratic rocks (phonolite, trachyte, augite syenite); open symbols are tephrite. Vertical bar represents estimated error at position of bar.

Figure 3 shows variation of the EAB rocks in terms of major-element concentrations *versus* distance along the belt as measured from Alamo Mountain at the northwestern end. Also plotted are the approximate locations of the Grenville Front and the PbTZ. I have chosen the Grenville Front as the dividing line between two segments along the trend, NW and SE, on the basis of chemical similarities.

Silica concentration (not recalculated on a volatile-free basis) in the leucocratic rocks shows the greatest variation in one group of intrusions in the NW segment. Variation in the NW segment decreases to the southeast. Samples with the lowest silica contents (within an intrusion or group of intrusions, these samples show the least amount of deuteric alteration and leaching) at each point on the trend show

increasing minimum  $\text{SiO}_2$  to the southeast. The increase is gradual in the NW segment, and the gradient increases at the Grenville Front as silica concentration increases toward about 320 km, where silica begins to drop off sharply. The inflection at 320 km is roughly coincident with the PbTZ. Alumina behaves in an antithetic manner.

The lack of systematic variation in Ca, Mg, and total iron (expressed as  $\text{Fe}_2\text{O}_3$ ) is exemplified by a plot of CaO (Fig. 3c). Concentrations of these elements are generally low or unsystematic northwest of the PbTZ, whereas each shows a systematic increase with distance to the southeast.

The variability of  $\text{Na}_2\text{O}$  and  $\text{K}_2\text{O}$  (Figs. 3d-e) is greatest in the NW segment. Sodium displays a greater range of variation within each intrusion, possibly due to sodium loss or mobilization during subsolidus vapor-phase crystallization or deuteritic alteration. The retention of sodium in late-stage liquids, and subsequent loss of sodium to vapor-phase or deuteritic alteration, have been suggested in the Cornudas Mountains (Barker *et al.* 1977), and elsewhere in both intrusive and extrusive peralkaline rocks. Variation of these two oxides is generally antithetic, potentially the result of the constant-sum effect, with relatively constant potassium concentration due to the "orthoclase effect" (Bailey & Schairer 1964). Most

variation in the concentration of the alkalis is a direct result of sodium loss (Barker *et al.* 1977). However, the molar ratio Na/K (Fig. 3f) shows a general southward decrease in the SE segment; the width of the swath of data within the SE segment is significantly smaller than the total variation present in individual intrusions of the NE segment. The cause of a southeastward decrease in sodium concentration is unknown.

Figure 4 shows normative mineralogy projected into the system  $\text{NaAlSi}_3\text{O}_8 - \text{KAlSi}_3\text{O}_8 - \text{SiO}_2$ . The EAB rocks fall on the trough connecting silica-undersaturated and -saturated minima in the system, and most samples cluster near the silica-saturated saddle on the undersaturated side of the  $\text{NaAlSi}_3\text{O}_8 - \text{KAlSi}_3\text{O}_8$  thermal divide. Barker *et al.* (1977) found that similar data for alkaline rocks of the Diablo Plateau (the same samples in some cases) plot on the saddle near the thermal divide, with the distance from the pseudoternary minimum the result of subsequent loss of mobile sodium in a late-stage vapor, or leaching by hydrothermal fluids as discussed above.

The peralkalinity of these rocks is expressed by the molar ratio  $(\text{Na} + \text{K})/\text{Al}$ . Of 67 leucocratic samples, 40 have values less than 1 (Table 1 and deposited documents). The maximum value of 1.2 is found in one sample, that of the chilled margin from Sierra Prieta (64 km). The next highest values are  $\sim 1.13$ , found in

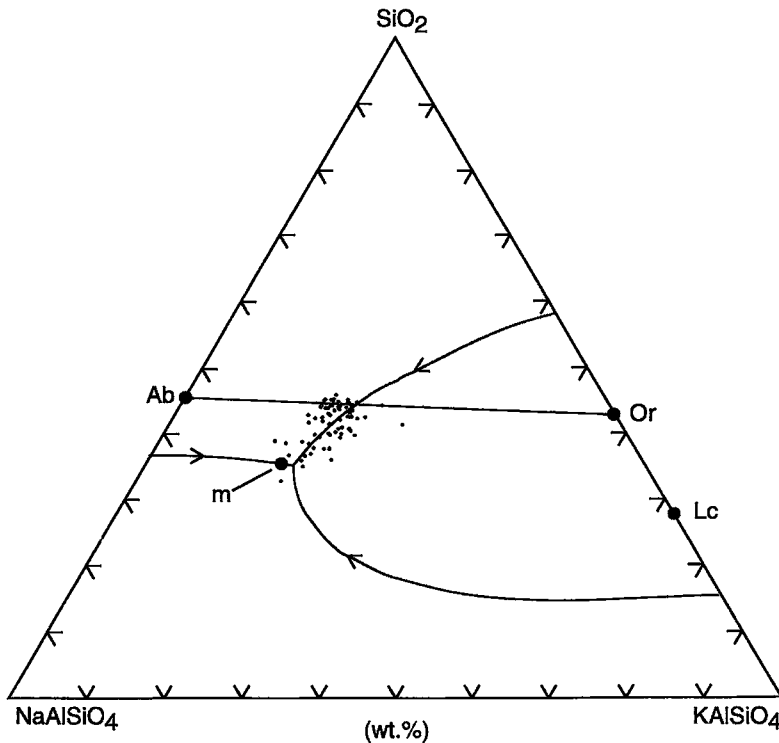


FIG. 4. EAB rocks projected into the system  $\text{NaAlSi}_3\text{O}_8 - \text{KAlSi}_3\text{O}_8 - \text{SiO}_2$ . Ternary undersaturated minimum (m) at 1 atm. from Schairer (1950).

the northwest Cornudas Mountains, the northern Davis Mountains (180 to 188 km), and at Black Mesa (304 km) in the PbTZ. The two samples of augite syenite (7 km) are the only leucocratic rocks in which this index is less than 0.85. The probable loss of sodium from the intrusions, as discussed above, is the likely cause of a lower-than-expected peralkaline index for these rocks. The presence of modal aenigmatite, arfvedsonite, and aegirine is strong evidence that these rocks were peralkaline before alteration, in spite of the low index of some samples.

#### Normalized element diagrams

Normalized element diagrams, or spidergrams (Thompson 1982), are presented here to draw specific conclusions relating to mineral behavior and to simplify subsequent discussion of the variation of certain elements. Figure 5 shows the Black Peak tephrite. It displays a relatively smooth concave-down shape with a high plateau (not a peak) between K and Ce. Slight and questionable positive anomalies in P and Ti may be the result of accumulation of apatite and titanian augite, both abundant in the rock. Plotted with the tephrite are average mid-ocean ridge basalt (MORB), average ocean-island basalt (OIB), and several published individual OIB patterns (Hofmann 1988, Fitton *et al.* 1991, Thompson *et al.* 1984). The patterns for OIB are a good match to the tephrite,

except that the tephrite spidergram is smoother than many published OIB patterns. The tephrite is not uniquely similar to OIB, having a pattern parallel to that of other continental alkaline basic rocks (Thompson *et al.* 1984), rift-related rocks from Kenya (Macdonald & Upton 1993), average Basin and Range basalts (Fitton *et al.* 1988), a Rio Grande Rift basanite (Gibson *et al.* 1992), nephelinite and basanite from western Germany (Wedepohl *et al.* 1994) and average Cameroon line basalts (Fitton & Dunlop 1985).

Leucocratic EAB rocks are plotted (Figs. 6a–f) with the tephrite for reference. Data for Cs have been added using a normalizing value of 0.017 (J.A. Wolff, pers. comm.) and placed on the spidergrams according to Sun (1980). Spidergrams of the leucocratic rocks are grouped by location. All display a hump centered between Rb and Ce, decreased levels of the middle rare-earths, and a second hump at Zr–Hf. The main hump is roughly convex in all samples except for those at the southeastern end of the NW segment (Fig. 6c) and all samples southeast of the PbTZ (Fig. 6f). Pronounced negative anomalies for Ba, Sr, P, and Ti were first noted in the NW segment by Forsythe & Nelson (1989) and can be directly related to compatible behavior by these elements (Thompson *et al.* 1984). In the EAB rocks, Sr, P, and Ba could be removed by apatite, plagioclase and alkali feldspar, and Ti could be removed as a component of titanian augite rather than ilmenite. The Black Peak tephrite contains abundant

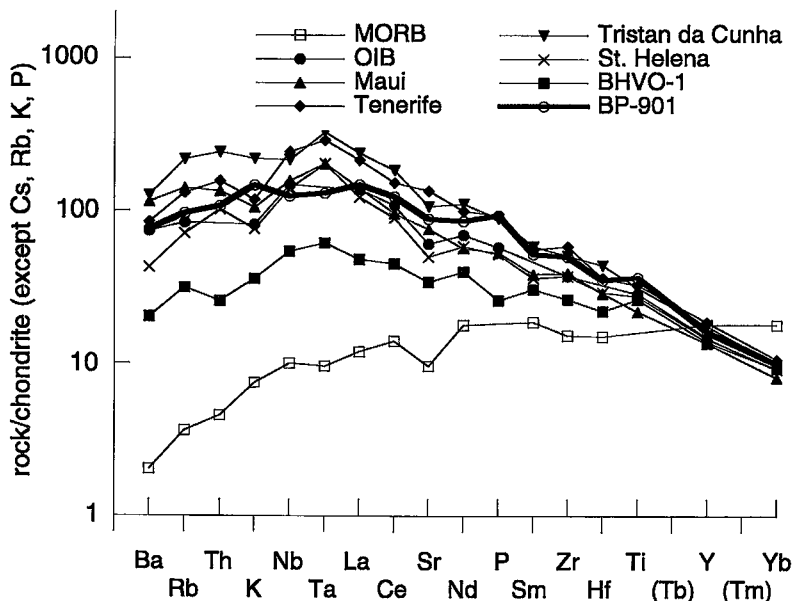


FIG. 5. Spidergrams of tephrite (BP-901), MORB average (Hofmann 1988), OIB average (Fitton *et al.* 1988), and selected OIB localities (Thompson *et al.* 1984), normalized to values suggested by Thompson (1982).

apatite, plagioclase, titanian augite and titaniferous magnetite. Regardless of which phases produced these anomalies, Ba, Sr, P, and Ti clearly behaved as compatible elements and should not be used in ratios with other more demonstrably incompatible elements. One pattern generally lacks these anomalies; the augite syenite from the NW segment most closely resembles that of the tephrite.

The roughly similar concentration of K in the leucocratic rocks is the possible result of alkali feldspar fractionation, leading to buffering of K by "cotectic equilibria in Petrogeny's Residua System" (Thompson *et al.* 1984). As discussed above, most of the leucocratic rocks project into the system  $\text{NaAlSi}_3\text{O}_8 - \text{KAlSi}_3\text{O}_8 - \text{SiO}_2$  on the cotectic near the silica-saturated saddle. Concentration of K may be constrained alternatively by the constant-sum effect, and small differences in the normalized concentration of this major (4 to 6%) element may not be obvious on a logarithmic scale (280 to 415).

Titanite phenocrysts are observed in several Eastern Rocky Mountain alkaline suites, including the Chico Sill Complex in northeastern New Mexico (Stobbe 1949), and the Rattlesnake Hills, Wyoming (Pekarek 1977). Titanite has not been reported in any EAB rock as a phenocryst, and has been reported in the border chill zones of two intrusions (Mayfield Valley and Marble Canyon; Barker *et al.* 1977, Price *et al.* 1986a) in a relationship that suggests reaction with carbonate wallrock. Titanite fractionation is therefore unlikely to exert a major control on the concentrations of trace elements in the leucocratic rocks. The depletion of Ta with respect to Nb as a direct result of titanite fractionation is well documented (Wolff 1984, Green & Pearson 1987, Weaver 1990). The normalized concentrations of Nb and Ta are subequal in most samples. The presence of titanite in the fractionating assemblage would cause a significant increase in Nb/Ta, which is not observed.

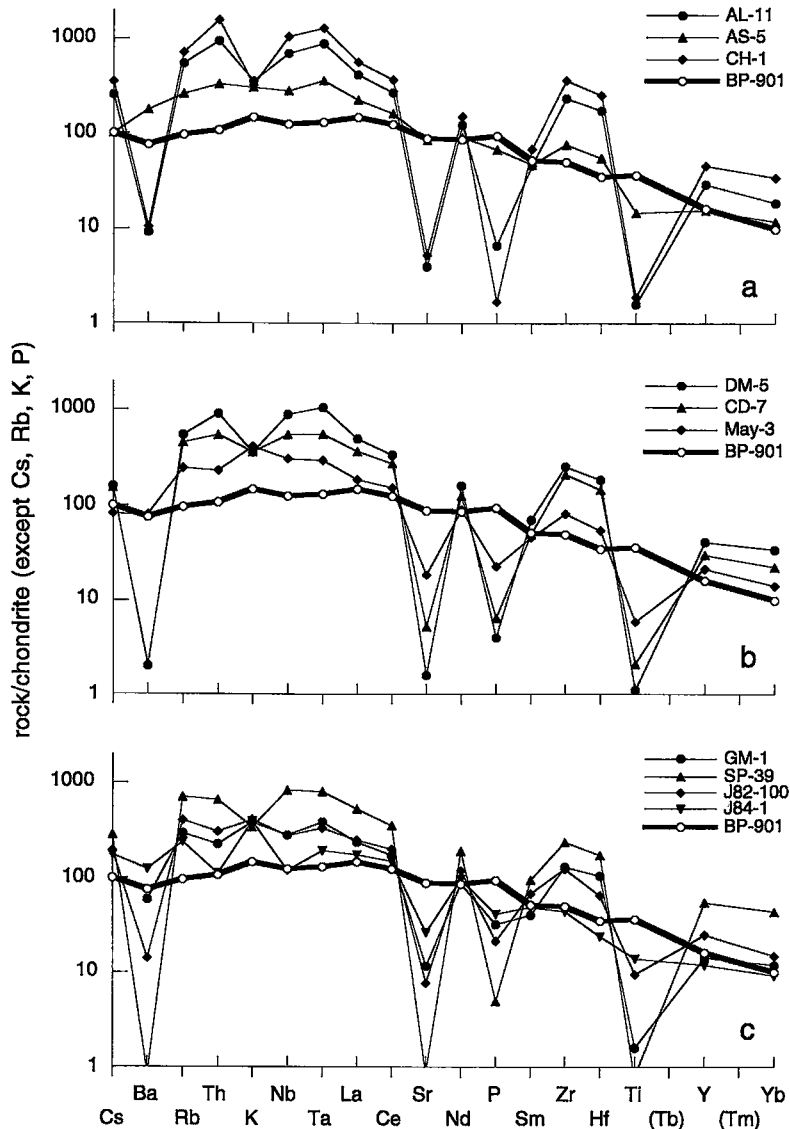
Zircon is likewise interpreted to have had no role in the fractionating assemblage. The increase in Zr solubility with increased alkalinity is well known (Watson 1979), and it is little surprise that no zircon has been reported from EAB rocks. In place of zircon are baddeleyite and a variety of complex Zr-silicates, such as eudialyte (*cf.* Barker & Hodges 1977, Boggs 1985), that have been observed as interstitial material in several of the phonolite specimens, especially by using combined back-scattered electron (BSE) imaging and energy-dispersion spectrometry (EDS) with the electron probe. On the spidergrams, the normalized ratio  $\text{Sm}/\text{Zr}$  decreases dramatically in the leucocratic EAB rocks with increasing overall concentrations of incompatible elements. Thompson *et al.* (1984) interpreted this as the result of removal of the middle rare-earths by apatite or other phases, whereas Zr was retained in the liquid.

Several investigators (Barker & Hodges 1977, Jones & Peckett 1980, Duggan 1988, Pearce 1989, Wolff & Toney 1993) have noted or discussed the incorporation of Zr into pyroxene and amphibole in peralkaline undersaturated rocks, in each case the probable result of suppression of zircon precipitation due to increased alkalinity or buffering by a halogen-rich vapor phase (*cf.* Bailey & Macdonald 1975). Sample BM-904 (at 304 km) contains aegirine, the bulk of which has a Zr concentration of less than 1 wt.%  $\text{ZrO}_2$ . The grains exhibit a thin outer zone on BSE images that contains approximately 7.5 %  $\text{ZrO}_2$ . The presence of measurable concentrations of Zr in pyroxene implies that the partition coefficient of Zr is not close to zero, yet the bulk of the Zr stayed in the liquid (or fluid) until near the end of crystallization, as indicated by the greatly concentrated zone at the rim.

Conspicuously absent from the spidergrams are significant negative anomalies at Nb and Ta (and concurrent high La/Nb) typical of subduction-related (*i.e.*, arc-related) melts, or those that contain components of continental crust (Wood *et al.* 1979, Saunders *et al.* 1980, Thompson 1982, Thompson *et al.* 1984, Hofmann 1988, Sun & McDonough 1989, Kelemen *et al.* 1993). The tephrite has high incompatible-element concentrations that are unlikely to be affected significantly by contamination following generation of the melt. If the tephrite is typical of mafic parental melts for these rocks, then the shape of spidergrams cannot be used to determine whether contamination has occurred following generation of the melt. Conversely, rocks that are trace-element-enriched should be good candidates for assessing the degree of contamination present in the source *prior* to melting. Lack of the Nb-Ta troughs in EAB rocks suggests that subduction inputs and continental crust have little, if any, role in the EAB source.

#### RARE-EARTH ELEMENTS

Figure 7 shows chondrite-normalized rare-earth-element (*REE*) patterns for the EAB rocks grouped geographically as in Figure 6. The leucocratic rocks produce a concave-upward pattern with a strong slope from the light to the middle rare-earths (*LREE* → *MREE*), negative Eu anomalies, and a generally flat or slightly concave-upward pattern between the *MREE* and heavy rare-earth elements (*HREE*). The chondrite-normalized ratio  $\text{Ce}_N/\text{Yb}_N$  ranges from 8 to 18. The NW segment hosts samples that are have the greatest  $\text{Ce}_N/\text{Yb}_N$  and greatest Eu anomalies ( $\text{Eu}/\text{Eu}^* = \text{Eu}_N/(\text{Sm}_N \cdot \text{Gd}_N)^{0.5} \approx 0.2$ ), primarily in the southern Cornudas Mountains (Fig. 7b). Samples from the SE segment display less variation in these *REE* parameters. Tephrite (Fig. 7e) displays a linear pattern with a slight positive Eu anomaly and  $\text{Ce}_N/\text{Yb}_N$  ranges from 12 to 14.



The variability in depth of the Eu trough may be suggestive of differing amounts of plagioclase, alkali feldspar or apatite fractionation, retention of Eu in the source, or changes in oxygen fugacity. Because the leucocratic intrusions have similar chemistry and mineral suites, I suggest that significant variation in intrinsic oxygen fugacity between intrusions is unlikely. The absence of a significant Eu anomaly in the tephrite and in three of the more primitive leucocratic rocks suggests that the anomalies are not a result of Eu fractionation in the source during melting.

The depletion of *MREE* may be the result of one or several contemporaneous processes. The scant literature on partition coefficients for *REE* in rocks of comparable composition (Larsen 1979, Wörner *et al.* 1983, Lemarchand *et al.* 1987, Weaver 1990) suggests that partition coefficients for apatite, clinopyroxene, and amphibole are an order of magnitude greater for *MREE* compared to the other *REE*. Moreover, apatite is an order of magnitude more efficient at concentrating *REE* than clinopyroxene or amphibole, with  $K^{Sm} \approx 100$  in both cases. Of the possible minerals responsible for concentration of *MREE*, clinopyroxene and amphibole

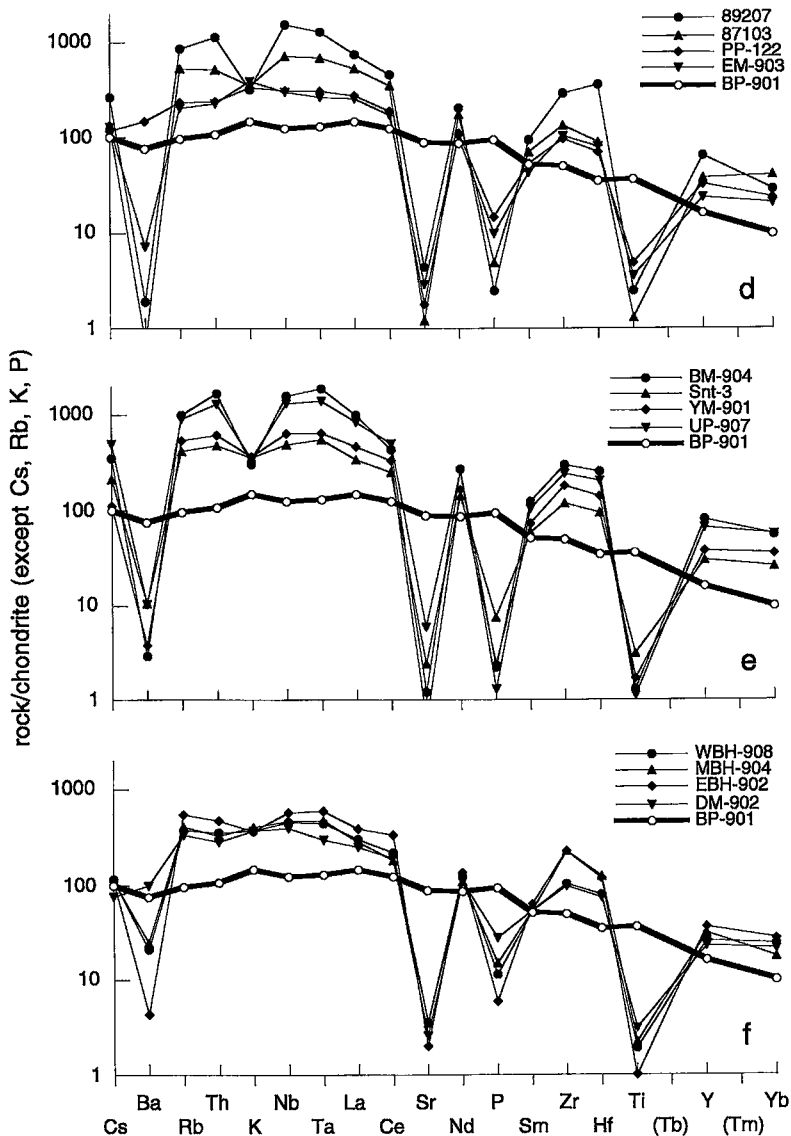


FIG. 6. Spidergrams of leucocratic EAB rocks [normalized to values of Thompson (1982); Cs value of 0.017 from J.A. Wolff, pers. comm.]. Thick line is tephrite, shown for comparison (BP-901, 321 km). Samples are listed by increasing distance from Alamo Mountain. a. Northern Cornudas Mountains (0 – 12 km). b. Southern Cornudas Mountains (18 – 27 km). c. Granite Mountain (43 km), Sierra Prieta (65 km), Marble Canyon dikes (94 km). d. Davis Mountains to Elephant Mountain (180 – 288 km). e. PbTZ (304 – 323 km). f. South of PbTZ (Black Hills, Dove Mountain; 335 – 352 km). Unpublished REE data for J82-100 and 89207 from C. Henry and D.F. Parker, respectively.

are too inefficient, although fractional crystallization of clinopyroxene certainly contributed to the *MREE* depletion. The straight-line pattern of two of the samples (at 27 and 94 km) suggests that apatite

fractionation may play a less important role in removing *MREE* at some localities, but apatite is interpreted as the primary agent for *MREE* removal within the belt.

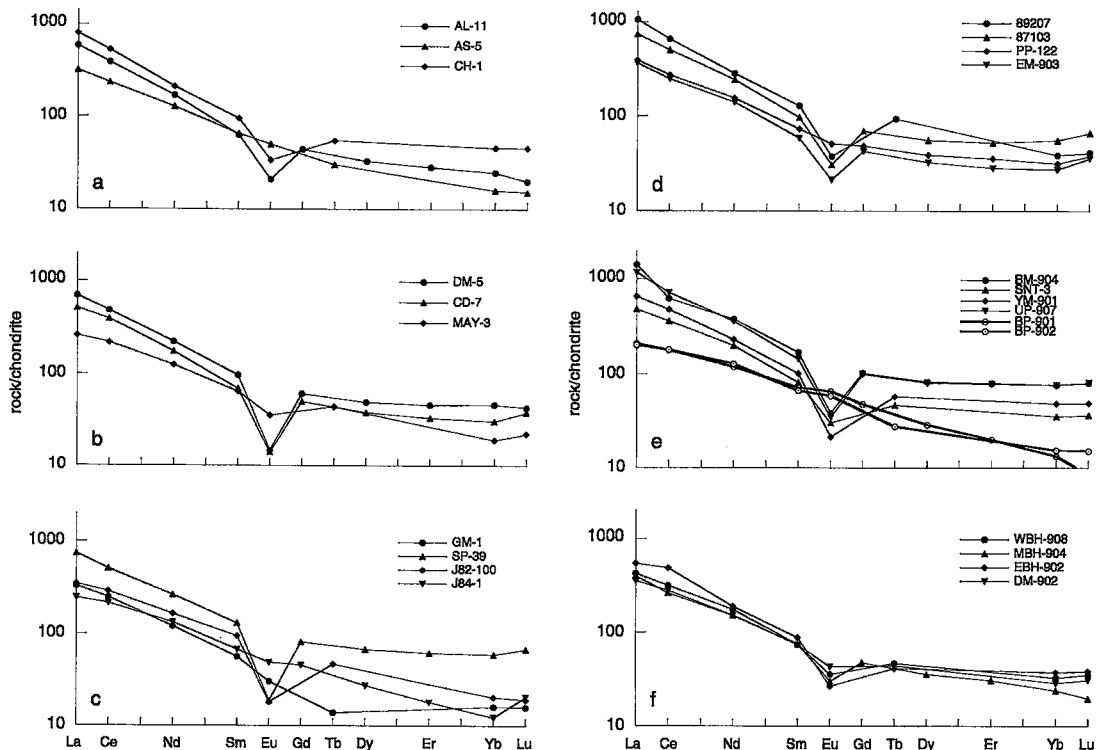


FIG. 7. REE concentrations, normalized to concentrations in chondrite (Anders & Grevesse 1989). Locations as for Figure 6. Samples BP-901 and BP-902 consist of tephrite.

#### GENERAL VARIATION ALONG STRIKE

As with the major elements, fractional crystallization and postcrystallization processes can produce dispersion within samples from the same intrusion. This results in "swaths" of data along the trend. Regional changes in chemistry commonly are subtle. For most elements, the greatest variation occurs in the southern part of the trend, at the approximate location of the PbTZ of James & Henry (1993a, b). The variations of trace-element concentrations (Sc, V, Cu, Zn, Rb, Sr, Y, Zr, Nb, Ba, Li, Cs, Hf, Ta, Th, U) *versus* strike distance are displayed in Data Repository figures, and selected examples are shown in Figure 8.

Plots of concentration *versus* distance (Fig. 8) produce similar patterns for several elements, including Zn, Rb, Y, Zr, Nb, Hf, Ta, Th, and U. Within the NW segment, the variation of these elements is described by significant variability and highest concentrations in the northwest, with variability decreasing to the southeast and overall low concentrations at 94 km. The 65-km samples produce a local anomaly with higher concentrations. The intrusions in the northern Davis Mountains (180 to 188 km) are clearly different. Systematic behavior resumes farther south in the SE

segment, with the exception of the highly differentiated intrusions at 304 and 323 km, and the tephrite, which increase the variability at the approximate location of the PbTZ. I interpret these patterns to depict the behavior of strongly incompatible elements. Thompson *et al.* (1984) suggested that, on the basis of published values available at the time, most of these elements have partition coefficients that are significantly above zero; the coherent increase in element concentrations over the OIB pattern is the result of the elements having the same level of bulk partitioning. In their opinion, the apparent total incompatibility (bulk partition-coefficient  $\approx 0$ ) of these elements is an illusion. Combined BSE imaging and EDS examination have allowed the recognition of several extremely fine-grained phases that serve as host to large quantities of otherwise incompatible elements within the groundmass of several samples. Phases recognized but not positively identified contain high concentrations of Zr (as described above), Nb, REE, and Th. Definitive identification of these mineral species is difficult owing to their small size (at or below analytical resolution of the electron beam), and low abundance. The important consideration here is that these elements were concentrated in these phases

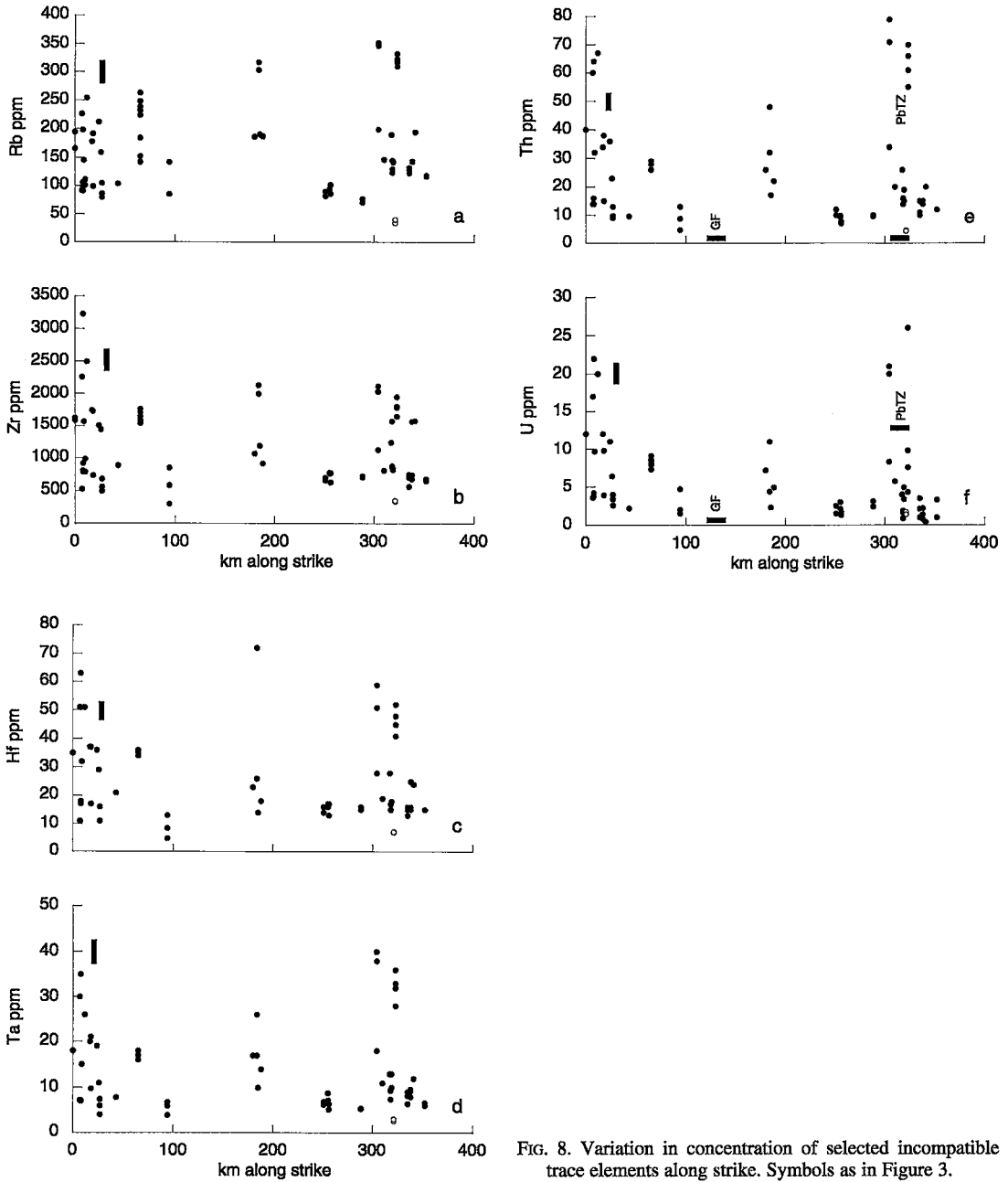


FIG. 8. Variation in concentration of selected incompatible trace elements along strike. Symbols as in Figure 3.

during groundmass crystallization or later, and therefore they were indeed incompatible.

#### ALKALI AND ALKALINE-EARTH ELEMENTS

The variations of Rb versus Sr and Ba (Figs. 9a, b) display patterns consistent with compatible behavior for the alkali earths and incompatible behavior for Rb.

These are comparable with the essentially L-shaped patterns produced by large degrees of crystal fractionation in silica-oversaturated magmas characterized by a very high Rb/Sr ratio (Halliday *et al.* 1993). Less scatter is observed in the Rb versus Ba plot. Direct connection between the tephrite and more evolved rocks is not demonstrable, owing to the lack of intermediate compositions. A plot of Sr versus Ba

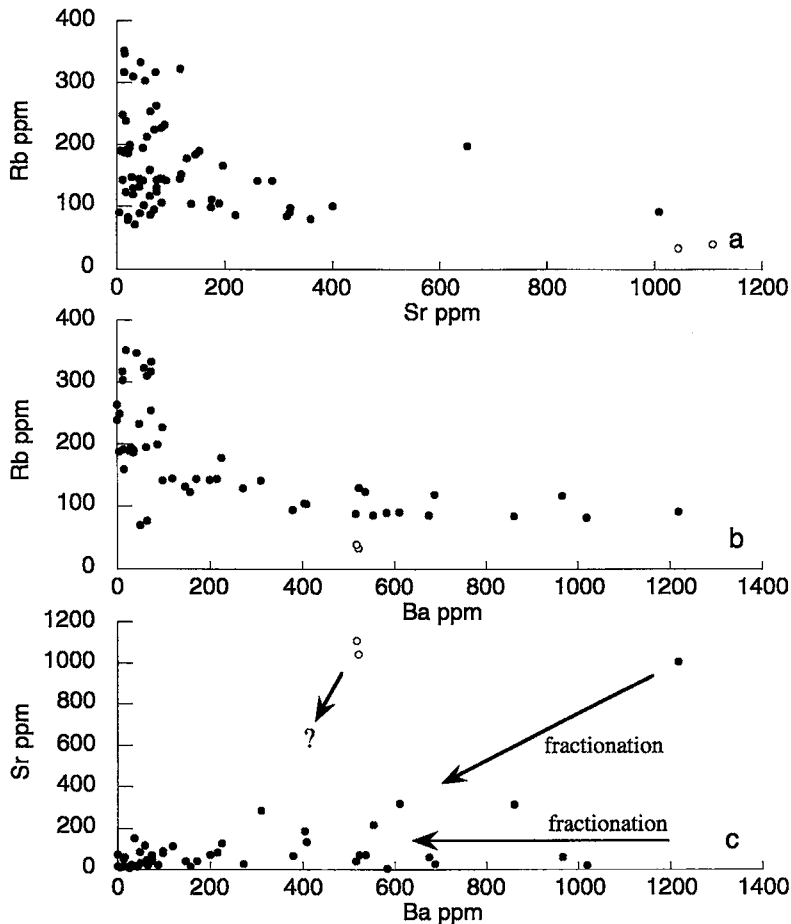


FIG. 9. Variation of Rb, Sr, and Ba concentrations. Arrows in Figure 9c show possible lines of descent from tephrite and other possible parental melts.

(Fig. 9c) suggests that the rocks that are highly depleted in these alkaline earths were generally derived from higher-Ba parents than the tephrite, with two converging lines of descent: high Sr in the NW segment, and low Sr, high Ba in the SE segment. A mafic parent with high Sr and relatively low Ba, like the tephrite, cannot account for all of the leucocratic EAB rocks.

Figure 10 shows Rb/Sr *versus* location; samples from the Diablo Plateau have greater variation than those from the Davis Mountains and south, with many samples in the range 1 to 5. The tephrite has a Rb/Sr in the range of 0.032 to 0.037. This is compatible with values of the primitive mantle, in the range 0.029 to 0.037 (Wood *et al.* 1979, Taylor & McLennan 1985, McDonough *et al.* 1992), with OIB values higher at 0.046. Some rocks in the NW segment have Rb/Sr < 1,

with minimum values increasing systematically southward to the end of the trend. All intrusions in the SE segment have Rb/Sr > 1. Maximum Rb/Sr is generally uniform (~25) along the trend, even in incompatible-element-enriched intrusions, and it is substantially lower than the values (100 to 10000) observed in some highly evolved silica-oversaturated (rhyolitic) systems (Halliday *et al.* 1993). Lower minimum Rb/Sr in the NW segment may be a result of better preservation of less-evolved melts, greater contamination by host carbonates, or contamination by a high-Sr, low-Rb crust underlying the NW segment. The NW segment is on a basement-cored uplift. The Central Basin Platform, located 2 degrees to the East, has been demonstrated to be at least partially cored by mafic intrusive complexes (Keller *et al.* 1989). Mafic rocks below the NW segment, if present, would provide a

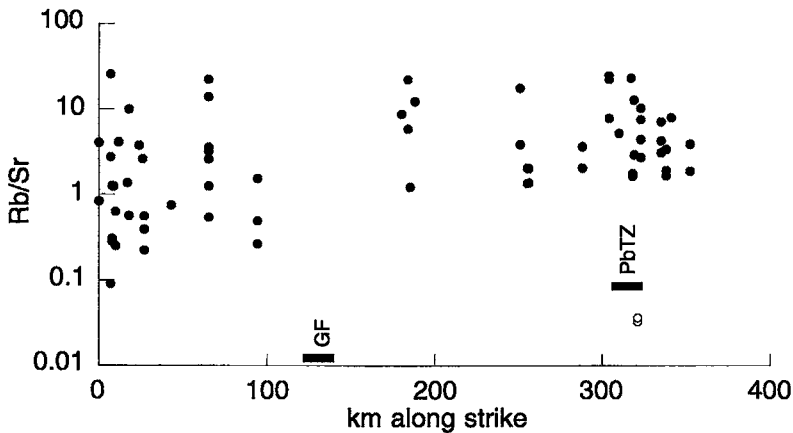


FIG. 10. Variation of Rb/Sr along strike.

major source for Sr contamination that would not increase silica contents. However, bulk contamination by carbonate was minuscule, as indicated by low concentrations of Ca and Sr in all of the leucocratic rocks. This information should be considered when interpreting Sr isotope data.

Jones & Drake (1993) examined the behavior of Rb and Cs in light of mass-balance considerations within the Earth and Moon. They concluded that Rb/Cs is  $\sim 80$  in both MORB and OIB sources, whereas the continental crust has a value of  $\sim 25$ . McDonough *et al.* (1994), in a review critical of Jones & Drake (1993), stated that a major reservoir had been ignored, and that ancient subducted crust, if properly accounted for, could lower the mantle values significantly. Estimates of Rb/Cs in the primitive mantle range from 20 to 45 (Wood *et al.* 1979, Sun 1980, Taylor & McLennan 1985, Hofmann 1988, McDonough *et al.* 1992). Leucocratic rocks within the EAB have Rb/Cs ranging from 30 to 150 (ignoring the extremely high and near-detection-limit samples), with the ratio in tephrite between 20 and 22, which corresponds well to a value of 19.8 in the primitive mantle (Hofmann 1988). Variation of Rb/Cs along strike (Fig. 11a) shows a constant decrease in the ratio toward the Grenville Front in the NW segment. The values of the ratio generally decrease in rocks south of the Davis Mountains, decreasing toward the tephrite, and increasing toward other rocks at the southern end of the trend. The lowest Rb/Cs rocks of the northern Davis Mountains could be construed as a continuation of the southward decreasing trend. The greatest variability is observed at the PbTZ, and no low values are observed south of the PbTZ. If the ratio of a presumably immobile high-field-strength element,

such as Th, against Cs is plotted against distance along the belt (Fig. 11b), the pattern is similar to that of Rb/Cs, but more pronounced.

Extreme sensitivity of Rb/Cs to loss of Cs has been noted in processes that involve fluids, such as alteration (Jones & Drake 1993) and subduction-related high-grade metamorphism. It is unclear whether the variability in the ratio is due to alteration, crystal fractionation, or some other process, and the means are currently unavailable to resolve this problem. One possible explanation is that the variation in Rb/Cs and Th/Cs can be related to the degree of partial melting of a depleted source. Cesium is included in several normalization schemes that have been proposed for the construction of spidergrams. It is always the most incompatible (left-most) of the elements, followed by Rb and Th (Ba is ignored in this discussion owing to its early removal by fractional crystallization). The Thompson (1982) scheme does not include Cs, but the normalization factor of 0.017 (J.A. Wolff, pers. comm.) produces a smooth curve for average MORB and OIB. Fitton & James (1986) demonstrated that decreasing degrees of partial melting (5% to 0.1%) of a depleted source would lead to spidergrams that not only show greater enrichment overall, but show greater curvature in their hump-shaped pattern. This will "draw out" the large-ion lithophile element (LILE) end of the pattern and separate Cs from Th more than Cs from Rb. Decreasing degrees of partial melting of the same depleted source will result in increases in both Rb/Cs and Th/Cs. If this analysis is correct, and if the relative compatibility of these elements remains unchanged during fractional crystallization, as is indicated by the smoothness of the spidergrams, then the patterns observed in Figure 11 are most likely the

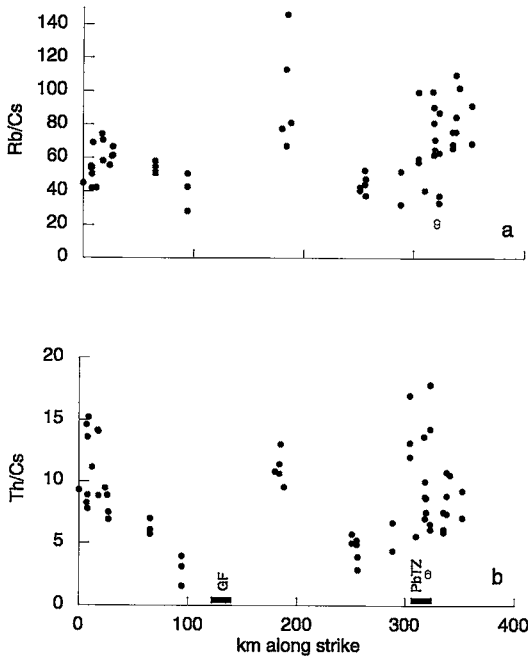


FIG. 11. Variation of Rb/Cs and Th/Cs along strike.

result of decrease in the degree of partial melting to the southeast in the NW segment, and a southeastward increase of same in the SE segment.

#### HIGH-FIELD-STRENGTH ELEMENTS

Figure 12a shows Th/U along strike. Rocks of the NW segment show little variation, having an average Th/U of 3.4, whereas the maximum value is 4.4. South of the Grenville Front, the minimum values in the leucocratic rocks increase slightly, and the total variability increases substantially at the PbTZ. Tephrite has a lower ratio (2.6 to 3.1). The chondritic value of the ratio is 3.62 (Anders & Grevesse 1989). Values for "normal" OIB averaged from several island complexes range from 3.54 to 3.78, whereas two islands interpreted as derived from enriched (EMI) mantle have Th/U of 4.50 to 4.86, just *slightly higher* (Weaver 1991). In the EAB rocks, the ratio is greatest in samples with the highest Th concentrations. Figure 12b displays concentrations of U *versus* Th. These two elements show a strong positive correlation up to the highest concentration of Th, where U falls off. I interpret this to be the probable result of oxidation of  $U^{4+}$  to  $U^{6+}$  and subsequent mobilization during deuteric alteration.

Much has been made of Zr/Nb in basic rocks from different tectonic settings (Pearce & Norry 1979,

Basaltic Volcanism Study Project 1981); the value of the ratio changes from 40 in normal MORB, to 10 in E-type MORB, to less than 10 in OIB rocks and rift settings (Africa's Western Rift:  $\sim 2$ ; Pearce & Norry 1979). The ratio shows little systematic variation with location along the belt, and ranges from 4 in the northern Davis Mountains, to as much as 10 in dikes at 94 km and at the PbTZ (Fig. 13a), whereas the ratio in tephrite is 7.7. Figure 13b displays concentrations of Nb *versus* Zr, which produces a strong positive correlation and two distinct trends defined by the samples with the highest concentration. Linear regression of samples north and south of the Grenville Front show that, within the scatter of the data, the NW segment has a higher average Zr/Nb. Few of the minerals present in EAB rocks are likely to alter Zr/Nb significantly during crystal fractionation; those that could are magnetite, ilmenite, and biotite (Pearce & Norry 1979, Weaver 1990).

Chondritic Zr/Hf is approximately 36, the same as most MORB and OIB (Anders & Grevesse 1989, Dupuy *et al.* 1992). Salters & Hart (1989) suggested that this consistency is the result of melting in the field of stability of garnet lherzolite. The average value of Zr/Hf (Fig. 14) in the EAB leucocratic rocks is 45 (48.8 in the tephrite), comparable to OIB from the

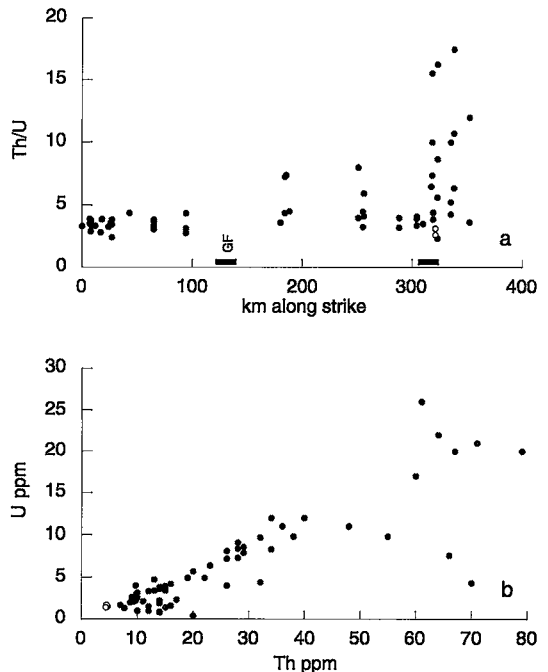


FIG. 12. Variation of Th and U concentrations, and of Th/U along strike.

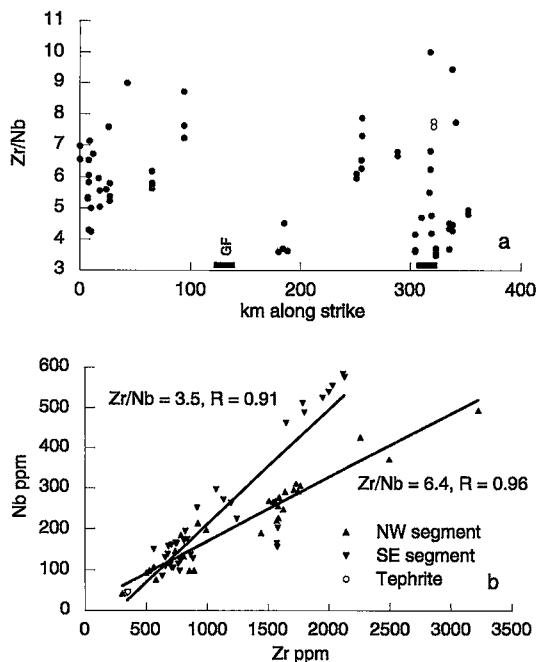


FIG. 13. Variation of Zr and Nb concentrations, and of Zr/Nb along strike.

South Atlantic (Weaver 1990). The deviation from chondritic values is best interpreted as a *loss* of Hf relative to Zr, as seen in Figures 5 and 6. Dupuy *et al.* (1992) listed basaltic rocks from intraplate ocean islands and continental settings that have higher than chondritic values of Zr/Hf, which they interpret as the result of heterogeneous mantle that is locally enriched by carbonate metasomatism. These authors state that "Zr/Hf may increase with differentiation in alkali suites"; a fractional crystallization process may explain the higher values observed locally within the belt (Fig. 14), but would not explain the high overall average of 45 for Zr/Hf.

Bau *et al.* (1994) suggested the incorporation of Zr in Mn-Fe nodules as a mechanism for enriching Zr in ocean-floor sediments such that the Zr/Hf is approximately 100. However, this reservoir seems to be volumetrically insignificant, considering that Zr concentration in these nodules is 228 ppm on average. This mechanism could explain a Zr enrichment, but not the Hf depletion observed in some OIB and continental alkaline magmas, and furthermore would require that an oceanic sediment component be added to the source.

The mobility of Zr and other "immobile" elements in peralkaline systems has long been recognized (Weaver *et al.* 1990, Vard & Williams-Jones 1993) and has been demonstrated in silica-oversaturated rocks of

the EAB (Rubin *et al.* 1993). The phonolite at 303 km exhibits some of the highest trace-element concentrations of the suite. It also contains numerous miarolitic cavities, which are generally penetrated by bladed crystals of aegirine. As discussed above, the clinopyroxene at this locality has a rim with  $\sim 7.5\%$   $ZrO_2$ . It was unclear during BSE imaging whether the grain examined was actually surrounded by matrix or by a soluble halide that is no longer extant, or whether it grew in a cavity. It is possible that the outermost Zr-rich zone is the result of crystallization from a halogen-rich fluid and not melt. No evidence of extensive fluid-rock reaction has been found in the host rocks; contact aureoles are reported to be  $\sim 1$  meter to a few meters thick. The ability of late-stage fluids to fractionate Hf from Zr is undocumented, but this mechanism should be considered as one possible control on Zr/Hf.

The lack of variation in Nb/Ta, discussed above, is highlighted in Figure 15, which shows a strong positive correlation. Three samples, all from the northern Davis Mountains intrusions, fall off the line, with higher Nb values. The chondritic Nb/Ta value is 17.3 (Anders & Grevesse 1989), approximately the same as the average value of  $16.6 \pm 2.6$  ( $n = 46$ ) obtained from Figure 15.

#### RELATIVE ROLES OF LITHOSPHERE AND ASTHENOSPHERE

Several models that explain the production of mafic melts in southwestern North America rely on an asthenospheric source for Basin and Range basalts and melts derived east of the Rio Grande Rift (Fitton *et al.* 1988, Leat *et al.* 1988, Kempton *et al.* 1991, Thompson *et al.* 1991, Gibson *et al.* 1992) similar to a source appropriate for ocean-island basalt. Other models suggest that an enriched lithospheric component is required to generate these intraplate alkaline melts

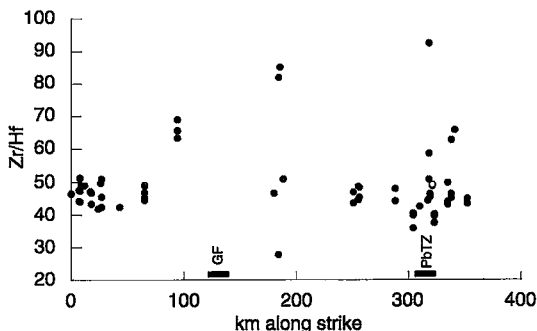


FIG. 14. Variation of Zr/Hf along strike.

(Perry *et al.* 1987, McDonough 1990). Detailed isotopic information, augmented by these trace-element data, is required for a realistic examination of the source of EAB melts, and for a discussion of origin of the EAB melts, in light of defined sources in the mantle, as was done by Zindler & Hart (1986) and Hart (1988). A suite of Pb and Nd isotopic data has been obtained with this goal in mind.

Figure 16 plots Th/Y *versus* Nb/Y and places the EAB rocks with MORB and OIB as asthenosphere-derived melts (Kempton *et al.* 1991). Also plotted are the loci of average upper and lower crust, and fields for Proterozoic supracrustal rocks and granulitic xenoliths from the Geronimo Field (G) (Kempton *et al.* 1991). Again, note that the EAB data trend away from crustal data of all types, and plot in the field of oceanic compositions. Without the isotopic information required for discussion of multiple sources in the mantle, it is reasonable to conclude that an asthenospheric component is the primary, and perhaps sole, progenitor of EAB magmas.

#### SUMMARY AND CONCLUSIONS

Phonolite and nepheline trachyte of the EAB display monotonously narrow ranges of ages and compositions in terms of major and selected trace elements along a belt more than 350 km long. What little variation is present is related to segments: the NW segment is underlain by Proterozoic rocks. The SE segment begins at the Grenville Front, and the basement is part of the Llano Terrane, which continues at least to the Ouachita Front. Trace-element concentrations and incompatible-element ratios change at the Grenville Front and the PbTZ of James & Henry (1993a, b) which is roughly coincident with the Ouachita Front. Leucocratic rocks north of the Grenville Front exhibit higher Rb/Sr and Zr/Nb values, lower Th/U values, and greater variability in element concentrations and ratios, which decreases toward the

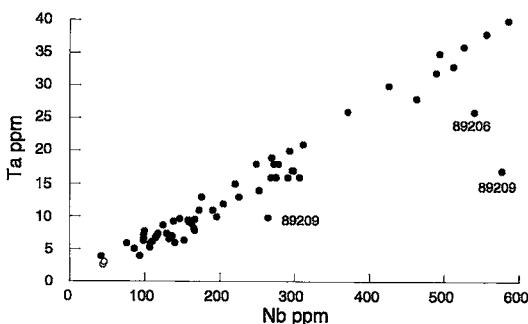


FIG. 15. Variation of Ta *versus* Nb concentrations.

boundary. Intrusions emplaced in the SE segment exhibit more overall variability and less systematic behavior in general. The greatest variability in most elements and element ratios is found at the PbTZ. In terms of the chemistry of the EAB rocks, it is unclear whether the PbTZ marks a distinct discontinuity in the basement, or whether it is simply the site of a slight change in the degree of partial melting or differentiation that is structurally controlled. Rocks of the northern Davis Mountains show chemical behavior for some high-field-strength elements (HFSE) that is not directly related to that of intrusions north or south along the trend. A tephrite intrusion in the EAB trend is a possible representative of the parental melt, but the lack of intermediate compositions makes this a tenuous connection, and possibly erroneous in light of variation among Rb, Sr, and Ba.

The normalized trace-element diagram of the EAB tephrite produced an OIB-like pattern, and this pattern is parallel to those of the leucocratic EAB rocks. Although subduction-related, these rocks show no evidence of significant modification by subduction processes, nor significant contamination by continental crust, despite their genesis beneath thick continental crust and high degrees of differentiation. The similarity to OIB is striking in light of constraints imposed by incompatible elements, and it persists despite extensive differentiation. Heterogeneities within the asthenospheric EAB source are minor in the area studied. Lower Rb/Sr values within the NW segment of the EAB suggest minor contamination by a Sr-rich reservoir, such as host carbonates or mafic crustal material, if contamination occurred at all.

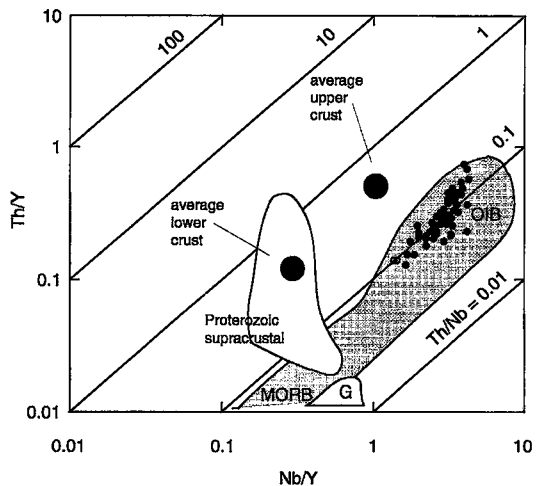


FIG. 16. Th/Y *versus* Nb/Y for EAB rocks (after Kempton *et al.* 1991). Field G: Geronimo crustal xenoliths. See text for discussion.

Compatible behavior by Ba, Sr, P, and Ti is observed to varying degrees, produced by a fractionating assemblage that likely contained plagioclase, apatite, titanite, and alkali feldspar. Zircon and titanite had no significant roles in the fractionating assemblage; *MREE* depletion was the result of varying degrees of apatite fractionation.

Several elements exhibit incompatible behavior; these include Rb, Y, Zn, Zr, Nb, Hf, Ta, Th, and U. Whereas it is unlikely that the bulk partition coefficients for these elements are near zero, they were primarily rejected from the crystallizing solid until crystallization of the last bit of liquid or fluid. This may be the result of complexing with chloride- or fluoride-rich fluids that did not escape by degassing, for example. Elements with multiple valence states (e.g., U) may have been mobilized during deuteric alteration relative to the more immobile HFSE (Th, Ta).

#### ACKNOWLEDGEMENTS

This research was supported in part by a Geological Society of America South-Central Section grant to Potter, and by generous contributions from the University of Texas Geology Foundation and Department of Geological Sciences. Daniel S. Barker, Chris Henry, and Don Parker provided some of the rock samples and access to unpublished data. The manuscript was greatly improved by thoughtful and thorough reviews of the original manuscript by D.S. Barker, G.N. Eby, J.G. Fitton, R.F. Martin, and D.F. Parker. I thank J. Gittins, L.L. Long, W.R. Muehlberger, and J.A. Wolff for their comments on this material during revision.

#### REFERENCES

- ANDERS, E. & GREVESSE, N. (1989): Abundance of the elements: meteoritic and solar. *Geochim. Cosmochim. Acta* **53**, 197-214.
- BAILEY, D.K. & MACDONALD, R. (1975): Fluorine and chlorine in peralkaline liquids and the need for magma generation in an open system. *Mineral. Mag.* **40**, 405-414.
- & SCHAIRER, J.F. (1964): Feldspar-liquid equilibria in peralkaline liquids – the orthoclase effect. *Am. J. Sci.* **262**, 1198-1206.
- BARKER, D.S. (1977): Northern Trans-Pecos magmatic province: introduction and comparison with the Kenya Rift. *Geol. Soc. Am., Bull.* **88**, 1421-1427.
- (1979): Cenozoic magmatism in the Trans-Pecos province: relation to the Rio Grande Rift. In *Rio Grande Rift: Tectonics and Magmatism* (R.E. Riecker, (ed.). American Geophysical Union, Washington, D.C. (382-392).
- (1987): Tertiary alkaline magmatism in the Trans-Pecos Texas. In *Alkaline Igneous Rocks* (J. Fitton & B.G.J. Upton, eds.). *Geol. Soc., Spec. Publ.* **30**, 415-431. Blackwell Scientific Publications, Oxford, U.K.
- & HODGES, F.N. (1977): Mineralogy of intrusions in the Diablo Plateau, northern Trans-Pecos magmatic province, Texas and New Mexico. *Geol. Soc. Am., Bull.* **88**, 1428-1436.
- , LONG, L.E., HOOPS, G.K. & HODGES, F.N. (1977): Petrology and Rb-Sr isotope geochemistry of intrusions in the Diablo Plateau, northern Trans-Pecos magmatic province, Texas and New Mexico. *Geol. Soc. Am., Bull.* **88**, 1437-1446.
- BASALTIC VOLCANISM STUDY PROJECT (1981): *Basaltic Volcanism on the Terrestrial Planets*. Pergamon Press, New York, N.Y.
- BAU, M., KOSCHINSKI, A. DULSKI, P. & HEIN, J. (1994): Y-Ho and Zr-Hf fractionation during hydrogenetic Fe-Mn crusts. *Berichte der Deutschen Mineral. Gesell.* **6**(1), 323 (abstr.).
- BLOOMFIELD, K. & CEPEDA-DAVILA, L. (1973): Oligocene alkaline igneous activity in NE Mexico. *Geol. Mag.* **110**, 551-555.
- BOGGS, R.C. (1985): Mineralogy of the Wind Mountain laccolith, Otero County, New Mexico. *New Mexico Geol.* **5**, 41-42.
- DENISON, R.E. & HETHERINGTON, E.A., JR. (1969): Basement rocks in far West Texas and south-central New Mexico. In *Border Stratigraphy Symposium* (F.E. Kottowski & D.V. Lemone, eds.). *New Mexico Bureau of Mines and Mineral Resources, Circ.* **104**, 1-16.
- DUGGAN, M.B. (1988): Zirconium-rich sodic pyroxenes in felsic volcanics from the Warrumbungle Volcano, central New South Wales, Australia. *Mineral. Mag.* **52**, 491-496.
- DUPUY, C., LIOTARD, J.M. & DOSTAL, J. (1992): Zr/Hf fractionation in intraplate basaltic rocks: carbonate metasomatism in the mantle source. *Geochim. Cosmochim. Acta* **56**, 2417-2423.
- ELIAS-HERRERA, M., RUBINOVICH-KOGAN, R., LOZANO-SANTA CRUZ, R. & SANCHEZ-ZAVALA, J.L. (1991): Nepheline-rich foidolites and rare-earth mineralization in the El Picacho Tertiary intrusive complex, Sierra de Tamaulipas, north-eastern Mexico. *Can. Mineral.* **29**, 319-336.
- FITTON, J.G. & DUNLOP, H.M. (1985): The Cameroon Line, West Africa, and its bearing on the origin of oceanic and continental alkali basalt. *Earth Planet. Sci. Lett.* **72**, 23-38.
- & JAMES D. (1986): Basic volcanism associated with intraplate linear features. *Phil. Trans., Roy. Soc.* **A317**, 253-266.
- , —————, KEMPTON, P.D., ORMEROD, D.S. & LEEMAN, W.P. (1988): The role of lithospheric mantle in the generation of late Cenozoic basic magmas in the western United States. *J. Petrol. (Spec. Vol.)*, 331-349.

- \_\_\_\_\_, \_\_\_\_\_ & LEE MAN, W.P. (1991): Basic magmatism associated with late Cenozoic extension in the western United States: compositional variations in space and time. *J. Geophys. Res.* **96**, 13693-13711.
- FLAWN, P.T. (1956): Basement rocks of Texas and southeast New Mexico. *Bureau of Economic Geology, University of Texas at Austin, Publ.* **5605**.
- \_\_\_\_\_, GOLDSTEIN, A., JR., KING, P.B. & WEAVER, C.E. (1961): The Ouachita System. *Bureau of Economic Geology, University of Texas at Austin, Publ.* **6120**.
- FORSYTHE, L.M. & NELSON, D.O. (1989): Geochemistry of Sierra Tinaja Pinata syenites, northern Diablo Plateau, Trans-Pecos, Texas. In Workshop on Geochemistry of Trans-Pecos Magmatism, Evolution of an Intercontinental Province (D.O. Nelson, comp.). *Department of Geology, Sul Ross State Univ., Alpine, Texas, Unpubl. Abstr.*, 16-19.
- GIBSON, S.A., THOMPSON, R.N., LEAT, P.T., DICKIN, A.P., MORRISON, M.A., HENDRY G.L. & MITCHELL, J.G. (1992): Asthenosphere-derived magmatism in the Rio Grande rift, western USA: implications for continental break-up. In *Magmatism and the Causes of Continental Breakup* (B.C. Storey, T. Alabaster & R.J. Pankhurst, eds.). *Geol. Soc., Spec. Publ.* **68**, 61-89. Blackwell Scientific Publications, Oxford, U.K.
- GILBERT, S.C. (1989): *Geochemical Contrasts between Nepheline Trachyte and Silica-Oversaturated Intrusive Igneous Rocks, Davis Mountains Volcanic Field, Trans-Pecos Texas*. B.S. thesis, Baylor University, Waco, Texas.
- GOETZ, L.K. & DICKERSON, P.W. (1985): A Paleozoic transform margin in Arizona, New Mexico, West Texas and Mexico. In *Structure and Tectonics of Trans-Pecos Texas* (P.W. Dickerson & W.R. Muehlberger, eds.). *West Texas Geol. Soc., Publ.* **85-81**, 173-184.
- GREEN, T.H. & PEARSON, N.J. (1987): An experimental study of Nb and Ta partitioning between Ti-rich minerals and silicate liquids at high pressure and temperature. *Geochim. Cosmochim. Acta* **51**, 55-62.
- HALLIDAY, A.N., DAVIDSON, J.P., HILDRETH, W. & HOLDEN, P. (1991): Modeling the petrogenesis of high Rb/Sr silicic magmas. *Chem. Geol.* **92**, 107-114.
- HANDSCHY, J.W., KELLER, G.R. & SMITH, K.J. (1987): The Ouachita System in northern Mexico. *Tectonics* **6**, 323-330.
- HART, S.R. (1988): Heterogeneous mantle domains: signatures, genesis and mixing chronologies. *Earth Planet. Sci. Lett.* **90**, 273-296.
- HENRY, C.D. & MCDOWELL, F.W. (1986): Geochronology and magmatism in the Tertiary volcanic field, Trans-Pecos, Texas. In *Igneous Geology of Trans-Pecos Texas* (J.G. Price, C.D. Henry, D.F. Parker & D.S. Barker, eds.). *Bureau of Economic Geology, University of Texas at Austin, Field Trip Guide and Research Articles, Guidebook* **23**, 99-122.
- \_\_\_\_\_, \_\_\_\_\_, PRICE, J.G. & SMYTH, R.C. (1986): Compilation of potassium-argon ages of Tertiary igneous rocks, Trans-Pecos, Texas. *Bureau of Economic Geology, University of Texas at Austin, Geol. Circ.* **86-2**.
- \_\_\_\_\_, PRICE, J.G. & JAMES, E.W. (1991): Mid-Cenozoic stress evolution and magmatism in the Southern Cordillera, Texas and Mexico: transition from continental arc to intraplate extension. *J. Geophys. Res.* **96**, 13545-13560.
- HOFMANN, A.W. (1988): Chemical differentiation of the Earth: the relationship between mantle, continental crust, and oceanic crust. *Earth Planet. Sci. Lett.* **90**, 297-314.
- JAMES, E.W. & HENRY, C.D. (1991): Compositional changes in Trans-Pecos Texas magmas coincident with Cenozoic stress realignment. *J. Geophys. Res.* **96**, 13561-13575.
- \_\_\_\_\_, \_\_\_\_\_ (1993a): Southeastern extent of the North American craton in Texas and northern Chihuahua as revealed by Pb isotopes. *Geol. Soc. Am., Bull.* **105**, 116-126.
- \_\_\_\_\_, \_\_\_\_\_ (1993b): Pb isotopes of ore deposits in Trans-Pecos Texas and northeastern Chihuahua, Mexico: basement, igneous and sedimentary sources of metals. *Econ. Geol.* **88**, 934-947.
- JONES, A.P. & PECKETT, A. (1980): Zirconium-bearing aegirines from Motzfeldt, South Greenland. *Contrib. Mineral. Petrol.* **75**, 251-255.
- JONES, J.H. & DRAKE, M.J. (1993): Rubidium and cesium in the Earth and the Moon. *Geochim. Cosmochim. Acta* **57**, 3785-3792.
- KELEMEN, P.B., SHIMIZU, N. & DUNN, T. (1993): Relative depletion of niobium in some arc magmas and the continental crust: partitioning of K, Nb, La and Ce during melt/rock reaction in the upper mantle. *Earth Planet. Sci. Lett.* **120**, 111-134.
- KELLER, G.R., HILLS, J.M. & BAKER, M.R. (1989): Geophysical and geochronological constraints on the extent and age of mafic intrusions in the basement of west Texas and eastern New Mexico. *Geology* **17**, 1049-1052.
- KEMPTON, P.D., FITTON, J.G., HAWKESWORTH, C.J. & ORMEROD, D.S. (1991): Isotopic and trace element constraints on the composition and evolution of the lithosphere beneath the southwestern United States. *J. Geophys. Res.* **96**, 13713-13735.
- KING, P.B. & FLAWN, P.T. (1953): Geology and mineral deposits of Pre-Cambrian rocks of the Van Horn area, Texas. *Bureau of Economic Geology, University of Texas at Austin, Publ.* **5301**.
- LAMBERT, D.D., MALEK, D.J. & DAHL, D.A. (1988): Rb-Sr and oxygen isotopic study of alkalic rocks from the Trans-Pecos magmatic province, Texas: implications for the petrogenesis and hydrothermal alteration of continental alkalic rocks. *Geochim. Cosmochim. Acta* **52**, 2357-2367.

- LARSEN, L.M. (1979): Distribution of REE and other trace elements between phenocrysts and peralkaline undersaturated magmas, exemplified by rocks from the Gardar igneous province, south Greenland. *Lithos* **12**, 303-315.
- LEAT, P.T., THOMPSON, R.N., MORRISON, M.A., HENDRY, G.L. & DICKIN, A.P. (1988): Compositionally-diverse Miocene–Recent rift-related magmatism in northwest Colorado: partial melting, and mixing of mafic magmas from 3 different asthenospheric and lithospheric mantle sources. *J. Petrol. (Spec. Vol.)*, 351-377.
- LE MAITRE, R.W., ed. (1989): *A Classification of Igneous Rocks and Glossary of Terms: Recommendations of the International Union of Geological Sciences, Subcommission on the Systematics of Igneous Rocks*. Blackwell Scientific Publ., Oxford, U.K.
- LEMARCHAND, F., VILLEMANT, B. & CALAS, G. (1987): Trace element distribution coefficients in alkaline series. *Geochim. Cosmochim. Acta* **51**, 1071-1081.
- LINDGREN, W. (1915): The igneous geology of the Cordilleras and its problems. In *Problems of American Geology: a Series of Lectures Dealing with some of the Problems of the Canadian Shield and of the Cordilleras* (delivered at Yale University on the Silliman Foundation in December, 1913) (W.M. Rice *et al.*, eds.). Yale University Press, New Haven, Connecticut (234-286).
- MACDONALD, R. & UPTON, B.G. (1993): The Proterozoic Gardar rift zone, south Greenland: comparisons with the East African Rift System. In *Magmatic Processes and Plate Tectonics* (H.M. Prichard, T. Alabaster, N.B.W. Harris & C.R. Neary, eds.). *Geol. Soc., Spec. Publ.* **76**, 427-442. Blackwell Scientific Publications, Oxford, U.K.
- MCDONOUGH, W.F. (1990): Constraints on the composition of the continental lithospheric mantle. *Earth Planet. Sci. Lett.* **101**, 1-18.
- \_\_\_\_\_, RINGWOOD, A.E., SUN, S.-S., JAGOUTZ, E. & HOFMANN, A.W. (1994): Comment on "Rubidium and cesium in the Earth and the Moon" by J.H. Jones and M.J. Drake. *Geochim. Cosmochim. Acta* **58**, 1385-1386.
- \_\_\_\_\_, SUN, S.-S., RINGWOOD, A.E., JAGOUTZ, E. & HOFMANN, A.W. (1992): Potassium, rubidium, and cesium in the Earth and Moon and the evolution of the mantle of the Earth. *Geochim. Cosmochim. Acta* **56**, 1001-1012.
- MCDOWELL, F.W. (1979): Potassium–argon dating in the Trans-Pecos Texas volcanic field. In *Cenozoic Geology of the Trans-Pecos Volcanic Field of Texas* (A.W. Walton & C.D. Henry, eds.). *Bureau of Economic Geology, University of Texas at Austin, Guidebook* **19**, 10-18.
- \_\_\_\_\_ & CLABAUGH, S.E. (1979): Ignimbrites of the Sierra Madre Occidental and their relation to the tectonic history of western Mexico. *Geol. Soc. Am., Spec. Pap.* **180**, 113-124.
- MOSHER, S. (1993): Western extension of Grenville age rocks; Texas. In *Precambrian: Conterminous U.S.* (J.C. Reed, Jr. *et al.*, eds.). *Geol. Soc. Am., The Geology of North America, DNAG Vol. C-2*, 365-378.
- MUEHLBERGER, W.R. & DICKERSON, P.W. (1989): A tectonic history of Trans-Pecos Texas. In *Structure and Stratigraphy of Trans-Pecos Texas* (W.R. Muehlberger & P.W. Dickerson, eds.). *Int. Geol. Congress, 28th, Field Trip Guidebook T317*. American Geophysical Union, Washington, D.C.
- NELSON, D.O. & NELSON, K.L. (1987): Geochemical comparison of alkaline volcanism in oceanic and continental settings; Clarion Island *versus* the eastern Trans-Pecos magmatic province. In *Mantle Metasomatism and Alkaline Magmatism* (E.M. Morris & J.D. Pasteris, eds.). *Geol. Soc. Am., Spec. Pap.* **215**, 317-333.
- PARKER, D.F. (1976): *Petrology and Eruptive History of an Oligocene Trachytic Shield Volcano, near Alpine, Texas*. Ph.D. thesis, Univ. of Texas at Austin, Austin, Texas.
- \_\_\_\_\_ (1983): Origin of the trachyte – quartz trachyte – peralkalic rhyolite suite of the Oligocene Paisano volcano, Trans-Pecos Texas. *Geol. Soc. Am., Bull.* **94**, 614-629.
- \_\_\_\_\_ & MCDOWELL, F.W. (1979): K–Ar geochronology of Oligocene volcanic rocks, Davis and Barrilla Mountains, Texas. *Geol. Soc. Am., Bull.* **90**, 1100-1110.
- PATCHETT, P.J. & RUIZ, J. (1987): Nd isotopic ages of crust formation and metamorphism in the Precambrian of eastern and southern Mexico. *Contrib. Mineral. Petrol.* **96**, 523-528.
- PEARCE, J.A. & NORRY, M.J. (1979): Petrogenetic implications of Ti, Zr, Y, and Nb variations in volcanic rocks. *Contrib. Mineral. Petrol.* **69**, 33-47.
- PEARCE, N.J.G. (1989): Zirconium-bearing amphiboles from the Igaliko dyke swarm, South Greenland. *Mineral. Mag.* **53**, 107-110.
- PEKAREK, A.H. (1977): The structural geology and volcanic petrology of the Rattlesnake Hills, Wyoming. *Wyoming Geol. Assoc. Earth Sci., Bull.* **10**(4), 1-30.
- PERRY, F.V., BALDRIDGE, W.S. & DEPAOLO, D.J. (1987): Role of asthenosphere and lithosphere in the genesis of late Cenozoic basaltic rocks from the Rio Grande Rift and adjacent regions of the southwestern United States. *J. Geophys. Res.* **92**, 9193-9213.
- POTTER, L.S. (1992): Trace element variation along strike in the Eastern Alkalic Belt, Trans-Pecos Magmatic Province, Texas and New Mexico. *Eos, Trans. Am. Geophys. Union, Abstr. Supplement* **73**, 658.
- \_\_\_\_\_ (1994): Influence of the North American Craton margin on chemical and isotopic variation along strike in the Eastern Alkalic Belt, Trans-Pecos Magmatic Province, Texas and New Mexico. *Geol. Assoc. Can. – Mineral. Assoc. Can., Program Abstr.* **19**, A89.
- \_\_\_\_\_ (1996): *Chemical and Isotopic Variation along Strike in the Eastern Alkalic Belt, Trans-Pecos Magmatic Province, Texas and New Mexico*. Ph.D. dissertation, University of Texas at Austin, Austin, Texas.

- PRICE, J.G. & HENRY, C.D. (1984): Stress orientations during Oligocene volcanism in Trans-Pecos Texas: timing the transition from Laramide compression to Basin and Range tension. *Geology* **12**, 238-241.
- \_\_\_\_\_, \_\_\_\_\_, BARKER, D.S. & PARKER, D.F. (1987): Alkalic rocks of contrasting tectonic settings in Trans-Pecos Texas. In *Mantle Metasomatism and Alkaline Magmatism* (E.M. Morris & J.D. Pasteris, eds.). *Geol. Soc. Am., Spec. Pap.* **215**, 335-346.
- \_\_\_\_\_, \_\_\_\_\_, \_\_\_\_\_ & RUBIN, J.N. (1986a): Petrology of the Marble Canyon Stock, Culbertson County, Texas. In *Igneous Geology of Trans-Pecos Texas. Field Trip Guide and Research Articles* (J.G. Price, C.D. Henry, D.F. Parker & D.S. Barker, eds.). *Bureau of Economic Geology, University of Texas at Austin, Guidebook* **23**, 303-319.
- \_\_\_\_\_, \_\_\_\_\_, PARKER, D.F. & BARKER, D.S., eds. (1986b): *Igneous Geology of Trans-Pecos Texas. Field Trip Guide and Research Articles. Bureau of Economic Geology, University of Texas at Austin, Guidebook* **23**.
- REED, J.C., JR., comp. (1993): Map of the Precambrian rocks of the conterminous United States and some adjacent parts of Canada. In *Precambrian: Conterminous U.S.* (J.C. Reed, et al., eds.). *Geol. Soc. Am., The Geology of North America, DNAG Vol. C-2*, Plate 1.
- ROBIN, C. & TOURNON, J. (1978): Spatial relations of andesitic and alkaline provinces in Mexico and central America. *Can. J. Earth Sci.* **15**, 1633-1641.
- RUBIN, J.N., HENRY, C.D. & PRICE, J.G. (1993): The mobility of zirconium and other "immobile" elements during hydrothermal alteration. *Chem. Geol.* **110**, 29-47.
- SALTERS, V.J.M. & HART, S.R. (1989): The hafnium paradox and the role of garnet in the source of mid-ocean-ridge basalts. *Nature* **342**, 420-422.
- SAUNDERS, A.D., TARNEY, J. & WEAVER, S.D. (1980): Transverse geochemical variations across the Antarctic Peninsula: implications for the genesis of calc-alkaline magmas. *Earth Planet. Sci. Lett.* **46**, 344-360.
- SCHAIERER, J.F. (1950): The alkali-feldspar join in the system  $\text{NaAlSi}_3\text{O}_8 - \text{KAlSi}_3\text{O}_8 - \text{SiO}_2$ . *J. Geol.* **58**, 512-517.
- STOBBE, H.R. (1949): Petrology of volcanic rocks of north-eastern New Mexico. *Geol. Soc. Am., Bull.* **60**, 1041-1093.
- SUN, S.-S. (1980): Lead isotopic study of young volcanic rocks from mid-ocean ridges, ocean islands and island arcs. *Phil. Trans., Roy. Soc. London* **A297**, 409-445.
- \_\_\_\_\_, & McDONOUGH, W.F. (1989): Chemical and isotopic systematics of ocean basalts: implications for mantle composition and processes. In *Magmatism in the Ocean Basins* (A.D. Saunders & M.J. Norry, eds.). *Geol. Soc., Spec. Publ.* **42**, 313-345.
- TAYLOR, S.R. & MCLENNAN, S.M. (1985): *The Continental Crust: its Composition and Evolution*. Blackwell, Oxford, U.K.
- THOMPSON, R.A., JOHNSON, C.M. & MEHNERT, H.H. (1991): Oligocene basaltic volcanism of the northern Rio Grande Rift: San Luis Hills, Colorado. *J. Geophys. Res.* **96**, 13577-13592.
- THOMPSON, R.N. (1982): British Tertiary volcanic province. *Scot. J. Geol.* **18**, 49-107.
- \_\_\_\_\_, MORRISON, M.A., HENDRY, G.L. & PARRY, S.J. (1984): An assessment of the relative roles of crust and mantle in magma genesis: an elemental approach. *Phil. Trans., Roy. Soc. London* **310**, 549-590.
- VARD, E. & WILLIAMS-JONES, A.E. (1993): A fluid inclusion study of vug minerals in dawsonite-altered phonolite sills, Montreal, Quebec: implications for HFSE mobility. *Contrib. Mineral. Petrol.* **113**, 410-423.
- WALKER, N. (1992): Middle Proterozoic geologic evolution of Llano uplift, Texas: evidence from U-Pb zircon geochronometry. *Geol. Soc. Am., Bull.* **104**, 494-504.
- WALTON, A.W. & HENRY, C.D., eds. (1979): *Cenozoic geology of the Trans-Pecos volcanic field of Texas. Bureau of Economic Geology, University of Texas at Austin, Guidebook* **19**.
- WATSON, E.B. (1979): Zircon saturation in felsic liquids: experimental results and applications to trace element geochemistry. *Contrib. Mineral. Petrol.* **70**, 407-419.
- WEAVER, B.L. (1990): Geochemistry of highly-undersaturated ocean island basalt suites from the South Atlantic Ocean: Fernando de Noronha and Trinidad islands. *Contrib. Mineral. Petrol.* **105**, 502-515.
- \_\_\_\_\_, (1991): The origin of ocean island basalt end-member compositions: trace element and isotopic constraints. *Earth Planet. Sci. Lett.* **104**, 381-397.
- WEAVER, S.D., GIBSON, I.L., HOUGHTON, B.F. & WILSON, C.J.N. (1990): Mobility of rare earth and other elements during crystallization of peralkaline silicic lavas. *J. Volcanol. Geotherm. Res.* **43**, 57-70.
- WEDEPOHL, K.H., GOHN, E. & HARTMANN, G. (1994): Cenozoic alkali basaltic magmas of western Germany and their products of differentiation. *Contrib. Mineral. Petrol.* **115**, 253-278.
- WOLFF, J.A. (1984): Variation of Nb/Ta during differentiation of phonolitic magma, Tenerife, Canary Islands. *Geochim. Cosmochim. Acta* **48**, 1345-1348.
- \_\_\_\_\_, & TONEY, J.B. (1993): Trapped liquid from a nepheline syenite: a re-evaluation of Na-Zr-F-rich interstitial glass in a xenolith from Tenerife, Canary Islands. *Lithos* **29**, 285-293.

- WOOD, D.A., JORON, J.L., TREUIL, M., NORRY, M. & TARNEY, J. (1979): Elemental and Sr isotope variations in basic lavas from Iceland and the surrounding ocean floor. *Contrib. Mineral. Petrol.* **70**, 319-339.
- WÖRNER, G., BEUSEN, J.-M., DUCHATEAU, N., GIBBELS, R. & SCHMINCKE, H.-U. (1983): Trace element abundances and mineral/melt distribution coefficients in phonolites from the Laacher See Volcano (Germany). *Contrib. Mineral. Petrol.* **84**, 152-173.
- ZINDLER, A. & HART, S. (1986): Chemical geodynamics. *Annu. Rev. Earth Planet. Sci.* **14**, 493-571.
- Received September 13, 1994, revised manuscript accepted February 4, 1996.*

## APPENDIX 1: SAMPLE NAMES, LOCATIONS, AND PREPARATION

Distance km	Sample	Prep	Intrusion Name	W Longitude	N Latitude
0.0	AL-11	1B	Alamo Mountain	105°38'	32°02'
0.0	AL-10	1B			
6.5	AS-5	1B	plug	105°33'	32°03'
6.5	AS-2	1B			
7.7	DE-1	1BP	Deer Mountain	105°33'	32°02'
7.7	DE-4	1B			
7.7	DE-5	1B			
7.4	Z-2	1BP	plug	105°33'	32°03'
8.6	WN-11	1BP	Wind Mountain	105°32'	32°02'
9.5	SA-12	1B	San Antonio Mtn.	105°33'	32°00'
12.0	CH-1	1BP	Chattfield Mountain	105°30'	32°00'
16.5	16M-2	1B	Sixteen Mountain	105°34'	31°55'
17.8	DM-3	1BP	Dog Mountain	105°31'	31°54'
17.8	DM-5	1BP			
24.2	Mit-2	1B	Miller Mountain	105°30'	31°52'
26.4	CD-7	1BP	Cerro Diablo	105°24'	31°54'
27.4	MAY-1B	1BP	Mayfield Valley	105°25'	31°52'
27.4	MAY-3	1BP			
27.4	MAY-4	1BP			
43.2	GM-1	1BP	Granite Mountain		
64.8	SP-3	1BP	Sierra Prieta	105°10'	31°34'
64.8	SP-20B	1B			
64.8	SP-20F	1B			
64.8	SP-22	1BP			
64.8	SP-28	1BP			
64.8	SP-39	1BP			
94.1	J82-100	2B	Marble Canyon	104°54'	31°26'
94.1	J82-103	2B			
94.1	J84-1	2B			
180.0	89208	3Pa	Horseshoe Butte	104°23'	30°42'
183.8	89207	3Pa	Brushy Mountain	104°21'	30°41'
183.8	89208	3Pa			
184.8	89209	3Pa	Baldy Mountain	104°22'	30°41'
187.7	87103	3Pa	El Muerto Peak	104°20'	30°40'
250.6	PP-3	4B	Paisano Peak	103°46'	30°19'
250.6	PP-122	4BP			
255.4	RP-2	4B	Ranger Peak	103°43'	30°17'
255.4	PP-358	4BP			
255.8	PP-158	4BP			
256.3	PP-159	4BP	Hunter's Cabin		
288.0	EM-803	P	Elephant Mountain	103°31.7'	30°01.99'
288.0	EM-806	P			
303.8	BM-801	P	Black Mesa	103°26.6'	29°53.7'
303.8	BM-802	P			
303.8	BM-804	P			
309.6	Snt-3	5B	Santiago Peak	103°25'	29°50'
317.3	YM-801	P	YE Mesa	103°20.5'	29°46.2'
318.2	SP-801	P	Sosa Peak	103°14.49'	29°52.22'
318.2	SP-803	P			
318.2	P-3	5B	(aka Puff's Peak)		
319.0	Ht-1	5B	Heart Mountain	103°15'	29°53'
319.0	Ht-2	5B			
320.9	BP-801	P	Black Peak	103°22.7'	29°43.2'
320.9	BP-802	P			
323.0	UP-804	P	unnamed Pope Ranch	103°12.32'	29°51.23'
323.0	UP-805	P		103°12.32'	29°51.23'
323.0	UP-806	P		103°12.32'	29°51.11'
323.0	UP-807	P		103°12.28'	29°51.16'
335.0	WBH-801	P	West Black Hill	103°01.8'	29°49.2'
335.0	WBH-807	P			
335.0	WBH-808	P			
338.4	MBH-801	P	Middle Black Hill	102°58.6'	29°49.15'
338.4	MBH-804	P		102°58.6'	29°48.98'
338.4	MBH-805	P		102°58.6'	29°49.05'
341.3	EBH-802	P	East Black Hill	102°58.71'	29°48.98'
352.3	DM-801	P	Dove Mountain	102°51.4'	29°45.0'
352.3	DM-802	P			

Preparation: P: collected by Potter, pulp in alumina ceramic shatterbox by Potter; B: D.S. Barker chips in steel jaw crusher ± disk mill; BP: chips by D.S. Barker, alumina ceramic shatterbox by Potter; Pa: D.F. Parker in WC shatterbox. References: 1 Barker *et al.* (1977), samples from D.S. Barker; 2 Price *et al.* (1986a), samples from C. Henry; 3 Gilbert (1989), samples from D.F. Parker; 4 Parker (1976) and Parker (1983), samples from D.F. Parker; 5 D.S. Barker (unpubl. data).